

Electronic Supplementary Information

Carbon-rich “Click” 1,2,3-Triazoles: Hexaphenylbenzene and Hexa-*peri*-Hexabenzocoronene-based Ligands for Suzuki-Miyaura Catalysts

*James R. Wright,^{ab} James D. Crowley,^{*a} and Nigel T. Lucas^{*ab}*

^aDepartment of Chemistry, University of Otago, PO Box 56, Dunedin, New Zealand.

^bMacDiarmid Institute for Advanced Materials and Nanotechnology, New Zealand.

Fax: +64 3 479 7906; Tel: +64 3 479 7731

*nlucas@chemistry.otago.ac.nz

*jcrowley@chemistry.otago.ac.nz

Contents

1	Experimental Procedures	3
2	CuAAC Optimisation Study for the Synthesis of Carbon-Rich Triazoles	13
3	^1H and ^{13}C NMR Spectroscopy	14
4	MALDI-TOF Mass Spectrometry	29
5	Ligand Donor Strength	32
6	X-ray Crystallography Data	33
7	Molecular Modelling.....	42
8	Catalyst Screening.....	46
9	References.....	48

1 Experimental Procedures

General

Unless otherwise stated, all reagents were purchased from commercial sources and used without further purification. Petroleum ether is the fraction of petrol boiling in the range 40–60 °C. All melting points were determined using a Mettler-Toledo FP62 apparatus and are uncorrected. ¹H NMR and ¹³C NMR spectra were recorded on a Varian 500 AR or Varian 400MR spectrometer at 25 °C and are referenced to CDCl₃ (7.26 ppm) and CDCl₃ (77.16 ppm), respectively, as reported by Gottlieb et al.¹ ¹H and ¹³C NMR spectra were assigned using 2D spectroscopies (COSY, NOESY, ¹H, ¹³C-HSQC, and ¹H, ¹³C-HMBC). ESI mass spectra were recorded on a Bruker MicrOTOF-Q mass spectrometer using a CH₂Cl₂ diluted into methanol. MALDI-TOF mass spectra were recorded on an Applied Biosystems 4800 Tandem TOF mass spectrometer with external calibration to within m/z ± 0.08; solid analyte and TCNQ matrix were mixed using a mini mixer-mill, suspended in hexane and transferred to the sample plate. Microanalyses were performed at the Campbell Microanalytical Laboratory, University of Otago. IR spectra were recorded neat on a Bruker AlphaP FTIR spectrometer with an attenuated total reflectance (ATR) module over the range 400–4000 cm⁻¹.

The precursors 4-(trimethylsilylethynyl)phenyl-penta(4-*tert*-butylphenyl)benzene (**HPB-alkyne-TMS**)² and 2-bromo-5,9,11,14,17-penta(*tert*-butyl)hexa-*peri*-hexabenzocoronene (**HBC-Br**),³ ligand 1-benzyl-4-phenyl-1*H*-1,2,3-triazole (**1c**),⁴ and complexes dichlorobis(acetonitrile)palladium(II),⁵ and **2c**⁴ were synthesised using literature synthetic procedures (or slight variations thereof).

Safety Note: Whilst no problems were encountered during the course of this work, azide compounds are potentially explosive and appropriate precautions should be taken when working with them.

Reaction Scheme for the Synthesis of HBC-alkyne

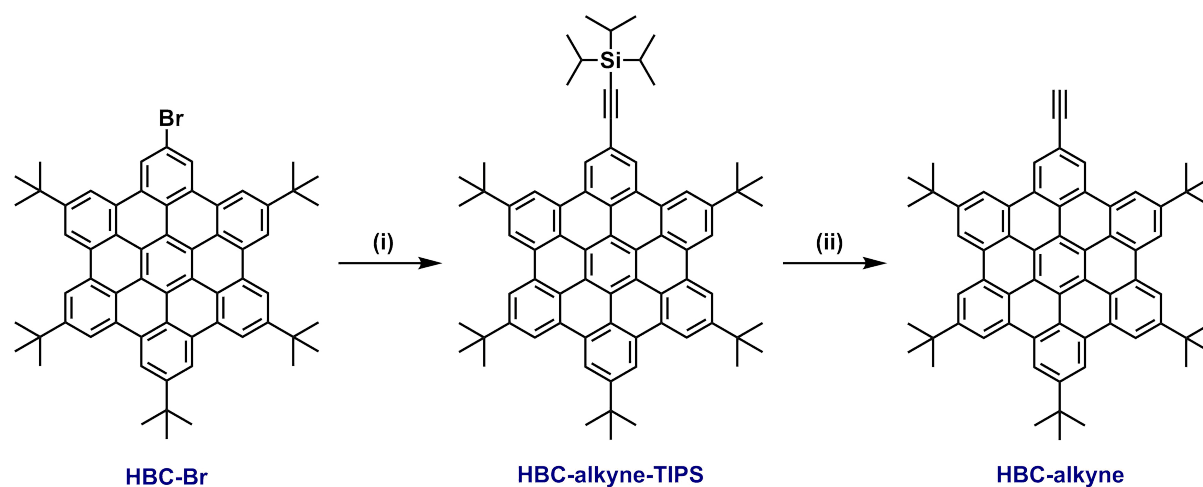
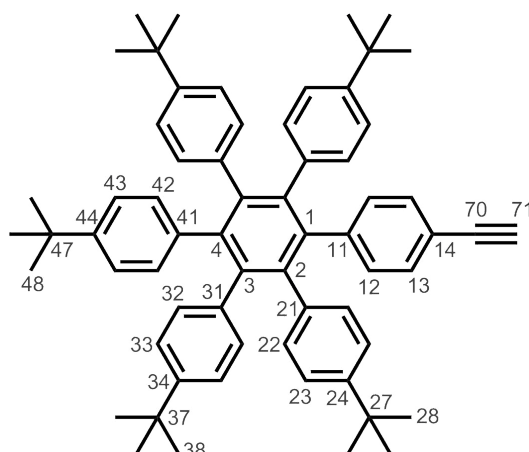


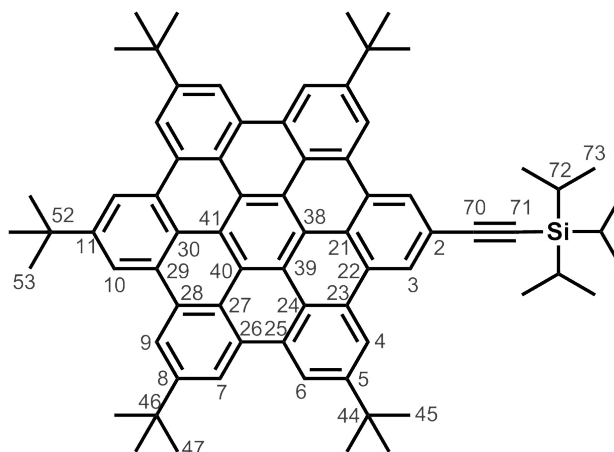
Figure 1.1 Conditions: (i) Triisopropylsilylacetylene (2.5 eq.), $[\text{PdCl}_2(\text{PPh}_3)_2]$ (0.06 eq.), CuI (0.15 eq.), piperidine, 75 °C, 18 hr, 91%; (ii) $[\text{nBu}_4\text{N}]\text{F}$ (1 mol L⁻¹ in THF, 1.5 eq.), CH_2Cl_2 , rt, 18 h, 88%.

Synthesis of HPB-alkyne



HPB-alkyne-TMS (0.452 mg, 0.49 mmol, 1.0 eq.) was dissolved in CH_2Cl_2 (100 mL). 1 mol L⁻¹ THF solution of tetra-*n*-butylammonium fluoride (TBAF, 0.75 mL, 0.74 mmol, 1.5 eq.) was added and the reaction mixture was stirred at rt for 1 h. The solvent was removed *in vacuo*. The reaction was redissolved in CH_2Cl_2 (60 mL) and washed with H_2O (3 × 50 mL), then brine (3 × 50 mL) and the solvent was removed *in vacuo* to afford the product as a white solid (414 mg, 98%). ¹H NMR (400 MHz, CDCl_3 , 298 K): δ 6.98 (d, $J = 8$ Hz, 2H, H₁₃), 6.84-6.78 (m, 12H, H_{12,23,33,43}), 6.68-6.63 (m, 10H, H_{22,32,42}), 2.92 (s, 1H, H₇₁), 1.12 (s, 18H, H₂₈), 1.09 (s, 27H, H_{38,48}) ppm. The ¹H NMR data of **HPB-alkyne** is consistent with data reported previously for this compound.²

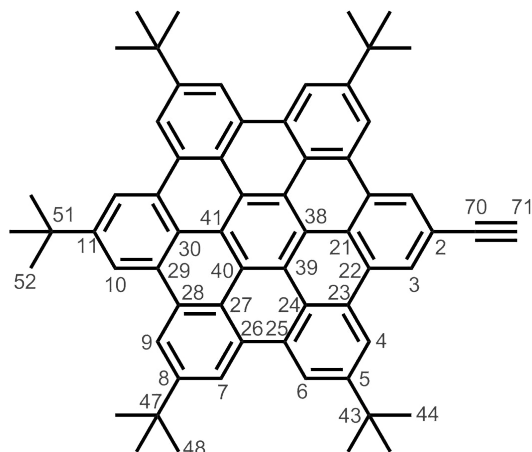
Synthesis of HBC-alkyne-TIPS



A Schlenk flask was charged with **HBC-Br** (0.304 g, 0.345 mmol, 1.0 eq.) and evacuated and backfilled (with argon) three times. Piperidine (20 mL) was added and the solution was deoxygenated with argon for 10 min. Triisopropylsilylacetylene (0.2 mL, 0.86 mmol, 2.5 eq.), copper(I) iodide (10 mg, 0.053 mmol, 0.15 eq.) and dichlorobis(triphenylphosphine)palladium(II) (16 mg, 0.022 mmol, 0.06 eq.) were added and the reaction was stirred under argon at 75 °C for 20 h. After cooling the reaction mixture was extracted into diethyl ether and washed with saturated NH₄Cl (3 × 50 mL), H₂O (3 × 50 mL), dried (MgSO₄) and the solvent was removed *in vacuo*. The mixture was purified by silica gel chromatography (10% CH₂Cl₂/petroleum ether) to afford HBC-alkyne as an orange solid (310 mg, 91%).

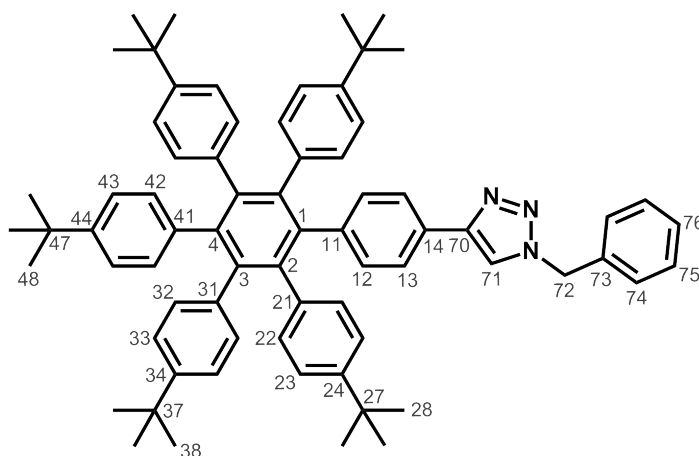
M.p. >230 °C. IR (ATR): ν = 2952, 2905, 2863, 2138 (C≡C), 1606, 1577, 1462, 1370, 1262, 1223, 1202, 987, 942, 866, 767, 746, 674, 631, 617 cm⁻¹. ¹H NMR (500 MHz, CDCl₃, 298 K): δ 9.10 (s, 2H, H₁₀), 9.07 (s, 2H, H_{7/9}), 9.04 (m, 2H, H_{7/9}), 9.00 (s, 2H, H₆), 8.88 (m, 4H, H_{3,4}), 1.91 (s, 9H, H₅₃), 1.88 (s, 18H, H₄₇), 1.85 (s, 18H, H₄₅), 1.41 (m, 21H, H_{72,73}) ppm. ¹³C NMR (126 MHz, CDCl₃, 298 K): δ 148.45 (C₁₁), 148.36 (C₅), 148.33 (C₈), 130.29 (C_{25/29}), 130.25 (C₂₂), 130.10 (C₂₈), 130.02 (C₂₆), 129.90 (C_{25/29}), 129.19 (C₂₃), 125.07 (C₂₁), 124.94 (C₃), 123.39 (C₃₀), 123.34 (C₂₇), 123.27 (C₂₄), 120.78 (C₃₈), 120.44 (C₄₁), 120.24 (C₄₀), 119.94 (C₃₉), 119.35 (C₂), 119.09 (C₄), 118.89 (C₆), 118.70 (C_{10,7/9}), 118.65 (C_{7/9}), 109.08 (C₇₀), 91.52 (C₇₁), 35.90 (C₅₂), 35.85 (C₄₆), 35.83 (C₄₄), 32.37 (C₅₃), 32.35 (C₄₇), 32.33 (C₄₅), 19.16 (C₇₃), 11.82 (C₇₂) ppm. MALDI-TOF (TCNQ): m/z = 982.57 [M]⁺, calc. 982.59. Elemental analysis calcd for C₇₃H₇₈Si: C 89.15, H 7.99; found C 88.73, H 7.88. Repeated elemental analyses consistently gave a low carbon composition, often seen for HBC compounds as a result of incomplete combustion.

Synthesis of HBC-alkyne



HBC-alkyne-TIPS (558 mg, 0.57 mmol, 1.0 eq.) was dissolved in CH_2Cl_2 (15 mL) to which was added 1 mol L^{-1} THF solution of TBAF (0.85 mL, 85 mmol, 1.5 eq.) and stirred at rt for 18 h. The solvent was removed *in vacuo* and purified by silica column chromatography (20% CH_2Cl_2 -petroleum ether) to obtain **HBC-alkyne** as an orange solid (411 mg, 88%). ^1H NMR (400 MHz, CDCl_3 , 298 K): δ 9.15 (s, 2H, H_{HBC}), 9.06 (s, 2H, H_{HBC}), 8.97 (s, 2H, H_{HBC}), 8.79 (s, 2H, H_{HBC}), 8.59 (s, 2H, H_{HBC}), 8.46 (s, 2H, H_{HBC}), 3.64 (s, 1H, H_{71}), 2.00 (s, 9H, H_{52}), 1.94 (s, 18H, H_{48}), 1.83 (s, 18H, H_{44}) ppm. The ^1H NMR data of **HBC-alkyne** is consistent with data reported previously for this compound.⁶

Synthesis of 1a

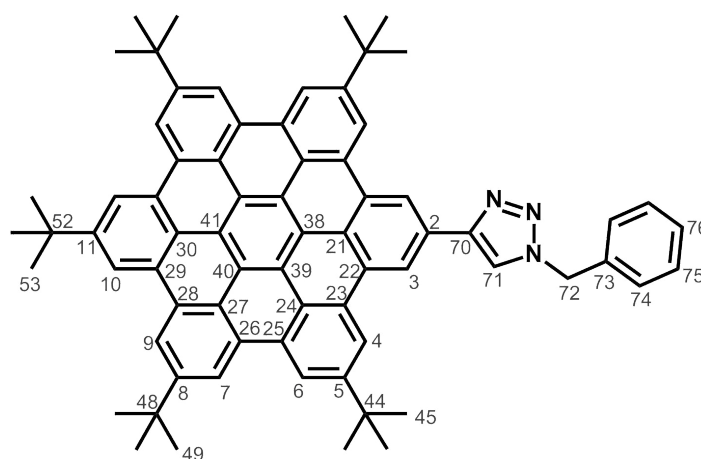


To CH_2Cl_2 (5 mL) was added tris(benzyltriazolylmethane) (TBTA) (27 mg, 0.051 mmol, 0.16 eq.), $[\text{Cu}(\text{CH}_3\text{CN})_4]\text{BF}_4$ (21 mg, 0.067 mmol, 0.22 eq.), benzyl azide (0.1 mL, 110 mg, 0.80 mmol, 2.6 eq.), NEt_3 (73 mg, 0.72 mmol, 2.3 eq.) and **HPB-alkyne** (257 mg, 0.31 mmol, 1.0 eq.) and the mixture stirred at rt for 18 h. The reaction mixture was washed with 0.1 M EDTA/ NH_4OH (2×40 mL), H_2O (2×40 mL), then dried (MgSO_4) and the solvent removed *in vacuo*. The residue was purified via silica chromatography (CH_2Cl_2), and **1a** isolated as a white solid (253 mg, 87%).

M.p. >230 °C. IR (ATR): $\nu = 3030, 2961, 2902, 2866, 1512, 1475, 1458, 1392, 1361, 1271, 1117, 1103, 1019, 863, 833, 779, 729, 720, 695, 682, 635, 626, 573$ cm^{-1} . ^1H NMR (500 MHz, CDCl_3 , 298 K): δ 7.38 (s, 1H, H_{71}), 7.37-7.34 (m, 3H, $\text{H}_{75,76}$), 7.27-7.25 (m, 4H, $\text{H}_{13,74}$), 6.90 (d, $J = 9$ Hz, 2H, H_{12}), 6.81-6.78 (m,

10H, H_{23,33,43}), 6.69 (d, *J* = 9 Hz, 4H, H₂₂), 6.69 (t, *J* = 8 Hz, 2H, H₄₂), 6.64 (d, *J* = 9 Hz, 4H, H₃₂), 5.48 (s, 2H, H₇₂), 1.09 (s, 27H, H_{38,48}), 1.07 (s, 18H, H₂₈) ppm. ¹³C NMR (125 MHz, CDCl₃, 298 K): δ 148.60 (C₇₀), 147.75 (C₂₄), 147.57 (C₄₄), 147.48 (C₃₄), 141.38 (C₁₁), 140.86 (C₃), 140.74 (C₄), 140.32 (C₂), 139.29 (C₁), 138.01 (C₄₁), 137.86 (C_{21/31}), 134.80 (C₇₃), 132.19 (C₁₂), 131.22 (C₂₂), 131.18 (C₄₂), 131.15 (C₃₂), 129.24 (C₇₅), 128.88 (C₇₆), 128.29 (C₇₄), 127.00 (C₁₄), 123.99 (C₁₃), 123.41 (C₂₃), 123.19 (C₄₃), 123.12 (C₃₃), 119.19 (C₇₁), 54.29 (C₇₂), 34.22 (C_{27/37}), 34.19 (C₄₇), 34.17 (C_{27/37}), 31.33 (C_{28,38,48}) ppm. HR-ESI-MS (CH₃OH/CH₂Cl₂): *m/z* = 1945.245 [2M+H]⁺, calc. 1945.234; 972.626 [M+H]⁺, calc. 972.619. MALDI-TOF (TCNQ): *m/z* = 994.57 [M+Na]⁺, calc. 994.60; 972.58 [M+H]⁺, calc. 972.62; 943.57 [M-N₂]⁺, calc. 943.61; 886.51 [M-N₂-^tBu]⁺, calc. 886.54; 852.52 [M-N₂-2(^tBu)+Na]⁺, calc. 852.46; 830.44 [M-N₂-2(^tBu)+H]⁺, calc. 830.47; 774.38 [M-N₂-3(^tBu)+2H]⁺, calc. 774.41. Elemental analysis calcd for C₇₁H₇₇N₃: C 87.70, H 7.98, N 4.32; found C 87.75, H 8.16, N 4.37.

Synthesis of **1b**

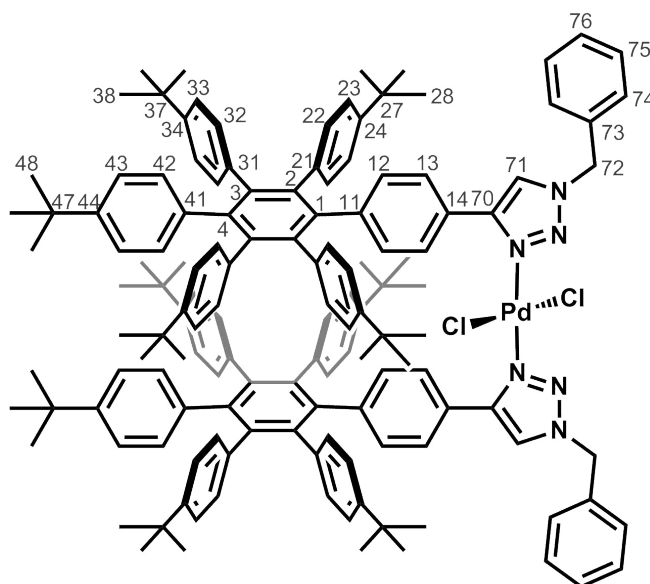


Method A: To CH₂Cl₂ (5 mL) was added TBTA (34 mg, 0.064 mmol, 0.11 eq.), [Cu(CH₃CN)₄]BF₄ (18 mg, 0.057 mmol, 0.10 eq.), benzyl azide (0.1 mL, 107 mg, 0.80 mmol, 1.4 eq.), NEt₃ (0.1 mL, 73 mg, 0.72 mmol, 1.2 eq.) and **HBC-alkyne** (478 mg, 0.58 mmol, 1.0 eq.) and stirred at rt for 18 h. The reaction mixture was washed with 0.1 M EDTA/NH₄OH (2 × 40 mL), H₂O (2 × 40 mL), then dried (MgSO₄) and the solvent was removed *in vacuo*. The product was purified via silica chromatography (CH₂Cl₂), and isolated as a bright yellow solid (384 mg, 69%).

Method B: A 3-necked round-bottom flask was fitted with a gas bubbler and an oil bubbler outlet. CH₂Cl₂ (20 mL) and **1a** (60 mg, 0.062 mmol, 1.0 eq.) were added and solution was purged with argon. After 5 min, a solution of FeCl₃ (240 mg, 1.5 mmol, 24 eq.) in CH₃NO₂ (2 mL) was added dropwise via a septum. The solution changed colour from colourless to dark red. The mixture was stirred for 30 min with continuous slow bubbling with argon. The reaction was quenched with CH₃OH (10 mL) causing a colour change from dark red to yellow, then the reaction mixture was washed with H₂O (2 × 20 mL) and dried (Na₂SO₄). After removing the solvents *in vacuo*, the crude was retreated using the same reaction conditions for 2 h. Using the same workup conditions resulted in a quantitative yield of **1b** as a yellow powder.

M.p. >230 °C. IR (ATR): $\nu = 3095, 3072, 3065, 2952, 2903, 2865, 1606, 1580, 1557, 1478, 1456, 1393, 1369, 1361, 1343, 1312, 1262, 1224, 1202, 1043, 1028, 941, 925, 887, 865, 812, 791, 746, 734, 720, 709, 696, 630, 610 \text{ cm}^{-1}$. ^1H NMR (500 MHz, CDCl_3 , 298 K): δ 9.53 (s, 2H, H₃), 9.25-9.23 (m, 10H, H_{4,6,7,9,10}), 8.26 (s, 1H, H₇₁), 7.52-7.48 (m, 4H, H_{74,75}), 7.44 (m, 1H, H₇₆), 5.82 (s, 2H, H₇₂), 1.83 (s, 27H, H_{49,53}), 1.80 (s, 18H, H₄₅) ppm. ^{13}C NMR (125 MHz, CDCl_3 , 298 K): δ 149.35 (C₇₀), 149.21 (C₅), 149.15 (C₁₁), 149.07 (C₈), 135.16 (C₇₃), 131.44 (C₂₂), 130.65 (C_{25,26,28,29}), 130.55 (C_{25,26,28,29}), 130.49 (C_{25,26,28,29}), 130.47 (C_{25,26,28,29}), 130.17 (C₂₃), 129.41 (C₇₅), 129.01 (C₇₆), 128.57 (C₂), 128.21 (C₇₄), 125.89 (C₂₁), 124.00 (C₂₄), 123.96 (C₃₀), 123.95 (C₂₇), 120.89 (C₄₁), 120.72 (C_{39/40}), 120.64 (C₇₁), 120.60 (C_{39/40}), 120.28 (C₃₈), 119.48 (C_H), 119.35 (C₃), 119.28 (C_H), 119.00 (C_H), 54.65 (C₇₂), 35.92 (C₄₄), 35.88 (C₅₂), 35.87 (C₄₈), 32.22 (C₄₅), 32.19 (C_{49,53}) ppm. MALDI-TOF (TCNQ): $m/z = 959.45 [\text{M}]^+$, calc. 959.52; 931.46 $[\text{M}-\text{N}_2]^+$, calc. 931.51; 916.56 $[\text{M}-\text{N}_2-\text{CH}_3]^+$, calc. 916.49. Elemental analysis calcd for C₇₁H₆₅N₃: C 88.80, H 6.82, N 4.38; found C 88.11, H 7.20, N 4.23. Repeated elemental analyses consistently gave a low carbon composition, often seen for HBC compounds as a result of incomplete combustion.

Synthesis of Palladium(II) Complex **2a**

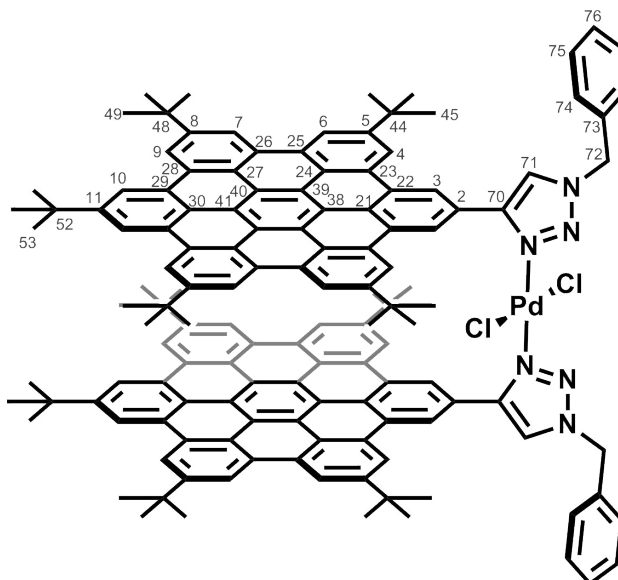


Triazole **1a** (92 mg, 0.09 mmol, 2 eq.) was suspended in acetone (5 mL). Bis(acetonitrile)dichloropalladium(II) (12 mg, 0.05 mmol, 1 eq.) dissolved in acetone (5 mL) was added dropwise to the triazole suspension. The reaction mixture was stirred for 2 h resulting in a colour change from orange to yellow. The solvent was removed *in vacuo*, then the reaction mixture was redissolved in a small amount of dichloromethane (approx. 3 mL), and purified by silica column chromatography (0-10% acetone/ CH_2Cl_2). The resulting yellow powder was washed with diethyl ether and filtered to obtain **2a** as yellow powder (63 mg, 63%).

M.p. >230 °C. IR (ATR): $\nu = 3034, 2961, 2903, 2863, 1511, 1498, 1472, 1458, 1392, 1361, 1271, 1150, 1117, 1104, 1018, 1001, 862, 833, 812, 801, 778, 730, 717, 683, 678, 635, 625, 573 \text{ cm}^{-1}$. ^1H NMR (500 MHz, CDCl_3 , 298 K): δ 7.40-7.36 (m, 6H, H_{75,76}), 7.32-7.30 (m, 4H, H₇₄), 7.24 (s, 2H, H₇₁), 6.86-6.60 (m, 48H, H_{HPB}), 5.53 (s, 4H, H₇₂), 1.08 (s, 18H, H₄₈), 1.09 (s, 36H, H₃₈), 0.97 (br s, 36H, H₂₈) ppm. ^{13}C NMR (125 MHz, CDCl_3 , 298 K) δ : 149.84 (C₇₀), 147.85 (C₂₄), 147.59 (C₄₄), 147.50 (C₃₄), 142.91 (C₁₁),

140.94 (C₄₀), 140.87 (C₃₀), 140.44 (C₂₀), 139.33 (C₁₀), 138.09 (C₃₁), 138.05 (C₄₁), 137.51 (C₂₁), 132.68 (C₄), 131.42-131.15 (C_{12,22,32,42}), 129.51 (C_{75,76}), 129.06 (C₇₄), 126.63 (C₁₄), 124.46 (C₁₃), 123.08 (C_{23,33,43}), 121.95 (C₇₁), 55.78 (C₇₂), 34.17 (C_{27,37,47}), 31.38 (C_{38,48}), 31.33 (C₂₈) ppm. MALDI-TOF-MS (TCNQ): $m/z = 2048.75$ [M-2Cl-H]⁺, calc. 2048.12. Elemental analysis calcd for C₁₄₂H₁₅₄Cl₂N₆Pd·0.5CH₂Cl₂: C 79.07, H 7.22, N 3.88; found C 78.97, H 7.27, N 3.99.

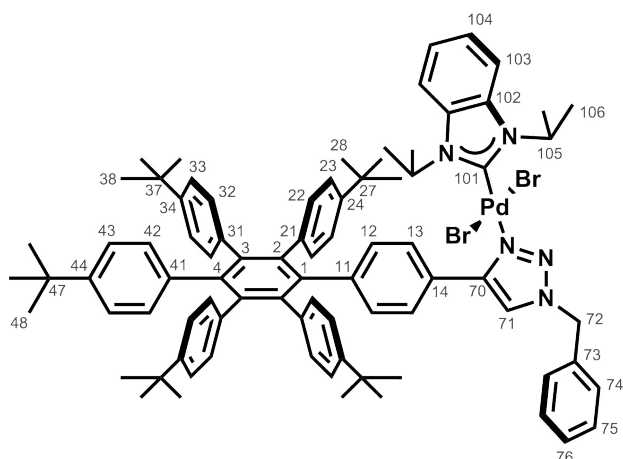
Synthesis of Palladium(II) Complex **2b**



Triazole **1b** (184 mg, 0.19 mmol, 2 eq.) was suspended in chloroform (5 mL). Bis(acetonitrile)dichloropalladium(II) (25 mg, 0.10 mmol, 1 eq.) was suspended in chloroform (5 mL) and added dropwise to the triazole solution. The reaction mixture was stirred for 1 h at rt. The solvent was removed *in vacuo*, the reaction mixture was redissolved in a small amount of dichloromethane (approx. 3 mL), and purified by silica column chromatography (CH₂Cl₂). After removal of solvent *in vacuo* complex **2b** was obtained as a bright yellow solid (172 mg, 86%).

M.p. >230 °C. IR (ATR): $\nu = 3071, 2954, 2903, 2865, 1607, 1580, 1477, 1459, 1425, 1392, 1364, 1346, 1264, 1225, 1201, 1109, 1023, 940, 925, 892, 867, 832, 797, 778, 746, 720, 697, 670, 630, 617, 572$ cm⁻¹. ¹H NMR (500 MHz, CDCl₃, 298 K): δ 9.87 (br s, 4H, H₃), 9.00 (s, 4H, H₄), 8.67 (m, 12H, H_{6,7/9,10}), 8.63 (s, 4H, H_{7/9}), 7.87 (s, 2H, H₇₁), 7.54 (m, 10H, H_{74,75,76}), 5.90 (s, 4H, H₇₂), 1.86 (s, 18H, H₅₃), 1.82 (s, 36H, H₄₉), 1.78 (s, 36H, H₄₅) ppm. ¹³C NMR (126 MHz, CDCl₃, 298 K) δ : 151.51 (C₇₀), 147.70 (C₅), 147.28 (C₁₁), 147.17 (C₈), 133.30 (C₇₃), 129.74 (C_{22/23/25/26/28/29}), 129.66 (C₇₅), 129.56 (C_{7/22/23/25/26/28/29}), 129.54 (C_{7/22/23/25/26/28/29}), 129.43 (C_{22/23/25/26/28/29}), 129.38 (C_{22/23/25/26/28/29}), 128.58 (C₇₄), 125.61 (C₂), 124.27 (C₂₁), 123.45 (C₇₁), 122.82 (C₂₄), 122.71 (C₃₀), 122.64 (C₂₇), 120.03 (C_{38/41}), 119.81 (C_{39/40}), 119.40 (C_{39/40}), 118.86 (C_{39/41}), 118.08-117.88 (C_H), 56.26 (C₇₂), 35.98 (C₄₄), 35.71 (C₅₂), 35.66 (C₄₈), 32.45 (C₅₃), 32.42 (C₄₉), 32.38 (C₄₅) ppm. MALDI-TOF-MS (TCNQ): $m/z = 2094.74$ [M]⁺, calc. 2094.88; 959.48 [L]⁺, calc. 959.52; 931.48 [L-N₂]⁺, calc. 931.52; 916.47 [L-N₂-CH₃]⁺, calc. 916.49. Elemental analysis calcd for C₁₄₂H₁₃₀Cl₂N₆Pd: C 81.30, H 6.25, N 4.01; found C 81.22, H 6.55, N 4.00.

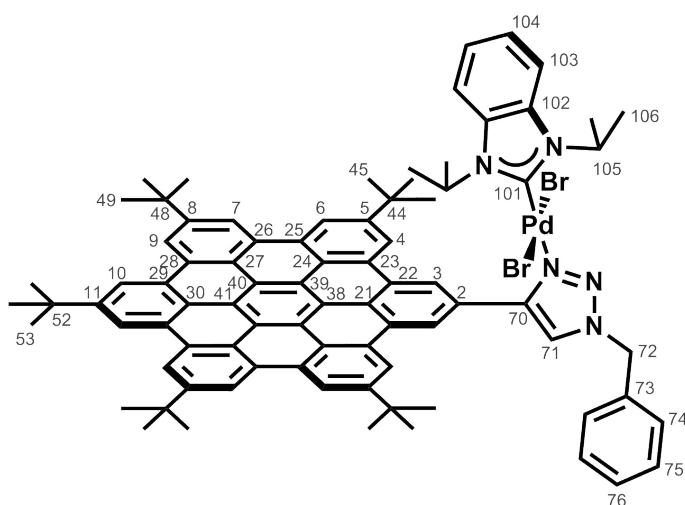
Synthesis of Palladium(II) Probe Complex 4a



Triazole **1a** (34 mg, 0.035 mmol, 1.0 eq.) and $[\text{PdBr}_2(\text{iPr-bimy})]_2$ (16 mg, 0.018 mmol, 0.5 eq.) were dissolved in CHCl_3 (10 mL) and heated at reflux for 3 h. After cooling the solvent was removed *in vacuo* to provide the product as a yellow solid in quantitative yield.

M.p. >230 °C. IR (ATR): $\nu = 3031, 2959, 2903, 2867, 1510, 1474, 1458, 1408, 1391, 1361, 1316, 1270, 1168, 1146, 1118, 1103, 1095, 1020, 860, 832, 778, 741, 730, 717, 677, 637, 625$ cm^{-1} . ^1H NMR (500 MHz, CDCl_3 , 298 K): 7.87 (br. m, 2H, H_{13}), 7.58 (m, 2H, H_{103}), 7.42-7.39 (m, 3H, $\text{H}_{6,7}$), 7.33 (m, 2H, H_5), 7.29 (s, 2H, H_2), 7.21 (m, 2H, H_{104}), 7.02 (d, $J = 9$ Hz, 2H, H_{12}), 6.83-6.79 (m, 10H, $\text{H}_{23,33,43}$), 6.71-6.64 (m, 10H, $\text{H}_{22,32,42}$), 5.56 (s, 2H, H_3), 1.80 (d, $J = 8$ Hz, 12H, H_{106}), 1.10 (s, 9H, H_{46}), 1.10 (s, 18H, H_{36}), 1.05 (m, 18H, H_{26}) ppm. ^{13}C NMR (126 MHz, CDCl_3 , 298 K): δ 149.35 (C_{70}), 147.92 (C_{24}), 147.63 (C_{44}), 147.53 (C_{34}), 140.94 (C_4), 140.92 (C_3), 140.40 (C_2), 139.12 (C_1), 138.01 ($\text{C}_{21,31,41}$), 137.49 (C_{11}), 133.67 (C_{102}), 132.92 (C_{73}), 131.16 ($\text{C}_{22,32,42}$), 129.52 (C_{75}), 129.45 (C_{76}), 129.08 (C_{74}), 126.61 (C_{13}), 125.60 (C_{14}), 123.70 (C_{23}), 123.22 (C_{43}), 123.16 (C_{33}), 122.21 (C_{104}), 121.82 (C_{71}), 112.72 (C_{103}), 55.45 (C_{72}), 54.67 (C_{105}), 34.24 (C_{25}), 34.21 (C_{45}), 34.18 (C_{35}), 31.34 ($\text{C}_{26,36,46}$), 20.97 (C_{106}) ppm; C_{101} not observed. MALDI-TOF-MS (TCNQ): $m/z = 1278.63$ [$\text{M}-2\text{Br}-\text{H}$] $^+$, calc. 1278.66. Elemental analysis calcd for $\text{C}_{84}\text{H}_{95}\text{Br}_2\text{N}_5\text{Pd}\cdot 0.3\text{CHCl}_3$: C 68.56, H 6.50, N 4.74; found C 68.45, H 6.50, N 4.61.

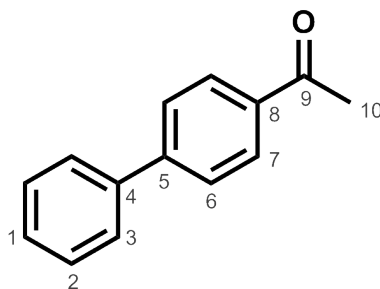
Synthesis of Palladium(II) Probe Complex **4b**



Triazole **1b** (34 mg, 0.035 mmol, 1 eq.) and $[\text{PdBr}_2(\text{iPr}_2\text{-bimy})]_2$ (16 mg, 0.018 mmol, 0.5 eq.) were dissolved in basic alumina-neutralized CHCl_3 (10 mL) and heated at reflux for 4 h. After cooling the solvent was removed *in vacuo* to provide the product as an orange solid in quantitative yield.

M.p. >230 °C. IR (ATR): $\nu = 3066, 2954, 2903, 2867, 1606, 1579, 1475, 1463, 1421, 1392, 1369, 1362, 1346, 1315, 1261, 1225, 1202, 1142, 1093, 941, 926, 888, 868, 740, 721, 697, 631$ cm^{-1} . ^1H NMR (500 MHz, CDCl_3 , 298 K): 9.75 (s, 2H, H_3), 9.43 (s, 2H, H_4), 9.34 (s, 2H, H_{10}), 9.33 (s, 2H, $\text{H}_{7/9}$), 9.31 (s, 2H, H_6), 9.31 (s, 2H, $\text{H}_{7/9}$), 7.98 (s, 1H, H_{71}), 7.62 (d, $J = 7$ Hz, 2H, H_{74}), 7.55 (t, $J = 7$ Hz, 2H, H_{75}), 7.50 (t, $J = 7$ Hz, 1H, H_{76}), 7.16 (m, 2H, H_{103}), 6.91 (m, 2H, H_{104}), 5.87 (s, 2H, H_{72}), 1.87 (s, 9H, H_{53}), 1.85 (s, 18H, H_{49}), 1.78 (s, 18H, H_{45}). The proton signals associated with the isopropyl groups were not observed, attributed hindered rotation about the ligand-metal bond. ^{13}C NMR (126 MHz, CDCl_3 , 298 K): δ 161.23 (C_{101}), 150.31 (C_{70}), 149.84 (C_5), 149.42 (C_{11}), 149.32 (C_8), 133.34 (C_{102}), 133.14 (C_{73}), 131.16 (C_{22}), 130.75 (C_{28}), 130.66 ($\text{C}_{25/29}$), 130.59 (C_{26}), 130.42 ($\text{C}_{25/29}$), 130.20 (C_{23}), 129.69 (C_{75}), 129.61 (C_{76}), 129.30 (C_{74}), 127.83 (C_2), 126.31 (C_{21}), 124.21 (C_3), 123.99 ($\text{C}_{24,27,30}$), 123.42 (C_{71}), 121.77 (C_{104}), 121.23 (C_{41}), 121.05 ($\text{C}_{39/40}$), 120.71 ($\text{C}_{39/40}$), 120.62 (C_4), 120.10 (C_{38}), 119.59 (C_6), 119.11 ($\text{C}_{7/9}$), 119.11 ($\text{C}_{7/9}$), 119.07 (C_{10}), 112.43 (C_{103}), 55.84 (C_{72}), 54.44 (C_{105}), 36.05 (C_{44}), 35.92 (C_{52}), 35.90 (C_{48}), 32.27 (C_{45}), 32.19 (C_{53}), 32.17 (C_{49}), 20.28 (C_{106}) ppm. MALDI-TOF-MS (TCNQ): $m/z = 1363.45$ $[\text{M}-\text{Br}+\text{OH}]^+$, calc. 1363.49; 1266.53 $[\text{M}-2\text{Br}-\text{H}]^+$, calc. 1266.56. Elemental analysis calcd for $\text{C}_{84}\text{H}_{83}\text{Br}_2\text{N}_5\text{Pd}$: C 70.61, H 5.86, N 4.90; found C 70.89, H 5.92, N 4.82.

Representative Procedure for the Synthesis of 4-acetylbiphenyl

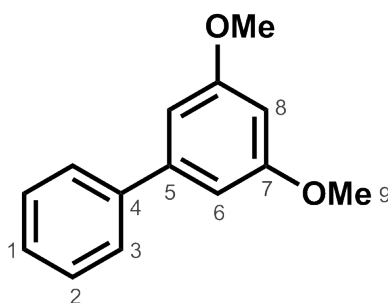


From 4-bromoacetophenone: A Schlenk flask was charged with K_2CO_3 (1.21 mmol, 2 eq.), phenylboronic acid (0.904 mmol, 1.5 eq.), 4-bromoacetophenone (0.603 mmol, 1 eq.) and internal standard 1,3,5-trimethoxybenzene (0.601 mol, 1.0 eq.). Solvents (toluene (16 mL), water (8 mL), *n*-propanol (4 mL)) were added and the solution was deoxygenated by bubbling with argon for at least 10 min. The catalyst (0.0301 mmol, 0.05 eq.) was added and the flask was lowered into a preheated oil bath (80 °C) and rapidly stirred for 4 h. The cooled reaction mixture was extracted into CH_2Cl_2 , and this organic layer was washed two times with distilled water, dried ($MgSO_4$) and the solvent was removed under reduced pressure to afford the crude product. The crude product was purified via column chromatography (1:1 dichloromethane/petrol) to afford the product as a white crystalline solid.

From 4-chloroacetophenone: 4-Chloroacetophenone (0.603 mmol, 1 eq.) was submitted to the same conditions as above for 4-bromoacetophenone for a reaction time of 30 h.

1H NMR (400 MHz, $CDCl_3$, 298 K): δ 8.04 (d, $J = 8$ Hz, 2H, H_7), 7.69 (d, $J = 8$ Hz, 2H, H_6), 7.63 (d, $J = 7$ Hz, 2H, H_3), 7.48 (t, $J = 7$ Hz, 2H, H_2), 7.41 (t, $J = 7$ Hz, 1H, H_1), 2.64 (s, 3H, H_{10}) ppm. ESI-MS (CH_2Cl_2/CH_3OH): $m/z = 219.076$ [$M+Na$] $^+$, calc 219.079. The 1H NMR and ESI-MS data for 3',5'-dimethoxybiphenyl are consistent with previous reports of the compound.⁷

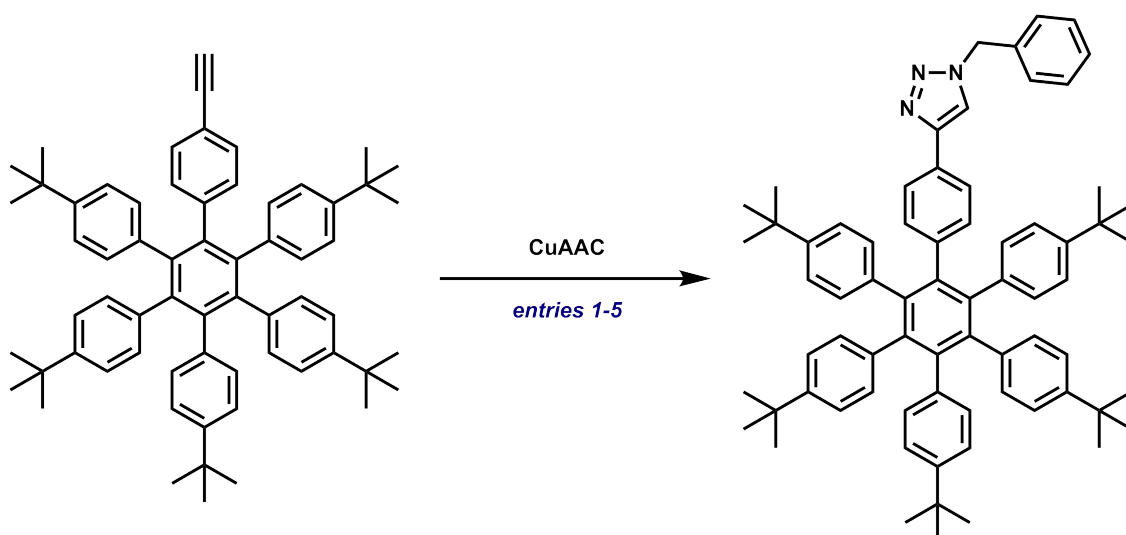
Representative Procedure for Synthesis of 3',5'-Dimethoxybiphenyl



A Schlenk flask was charged with K_2CO_3 (1.21 mmol, 2 eq.), phenylboronic acid (0.904 mmol, 1.5 eq.), 3,5-dimethoxybromobenzene (0.603 mmol, 1 eq.) and internal standard 1,3,5-trimethoxybenzene (0.601 mol, 1.0 eq.). The solvents (toluene (16 mL), water (8 mL), *n*-propanol (4 mL)) were added and the solution was deoxygenated with argon for at least 10 min. The catalyst (0.0301 mmol, 0.05 eq.) was added and the flask was lowered into a preheated oil bath (80 °C) and rapidly stirred for 4 h. The

cooled reaction mixture was extracted into CH_2Cl_2 , and the organic layer washed two times with distilled water, dried (MgSO_4) and the solvent was removed under reduced pressure to afford the crude product. The crude product was purified via column chromatography (1:1 dichloromethane/petrol) to afford the product as a white crystalline solid. ^1H NMR (400 MHz, CDCl_3 , 298 K) : δ 7.58 (d, $J = 7$ Hz, 2H, H_3), 7.44 (t, $J = 7$ Hz, 2H, H_2), 7.36 (t, $J = 7$ Hz, 1H, H_1), 6.74 (d, $J = 2$ Hz, 2H, H_6), 6.48 (t, $J = 2$ Hz, 1H, H_8), 3.86 (s, 6H, H_9) ppm. ESI-MS ($\text{CH}_2\text{Cl}_2/\text{CH}_3\text{OH}$): $m/z = 215.105$ $[\text{M}+\text{H}]^+$, calc. 215.107. The ^1H NMR and ESI-MS data for 3',5'-dimethoxybiphenyl are consistent with previous reports of the compound.⁸

2 CuAAC Optimisation Study for the Synthesis of Carbon-Rich Triazoles



Entry	Eq. BnN_3	Eq. Base	Eq. 'Cu'	Eq. TBTA	Solvent	Time (h)	Yield ^h
1	1.1 ^a	1.2 ^d	0.5 ^f	-	THF/ H_2O (4:1)	24	0
2	3.8 ^b	-	2.5 ^f	-	THF/DMF/ H_2O (4:4:1)	24	0
3	1.1 ^b	-	1.5 ^f	1.1	THF/DMF/ H_2O (4:4:1)	6	25
4	1.1 ^b	-	1.1 ^g	1.1	CH_2Cl_2 /DMF (2:1)	24	35
5	1.5^c	1.1^e	0.1^g	0.1	CH_2Cl_2	15	90

^a BnN_3 formed *in situ* (BnBr/NaN_3). ^b BnN_3 as DMF solution. ^c BnN_3 neat. ^d Na_2CO_3 . ^e NEt_3 . ^f $\text{CuSO}_4 \cdot 5\text{H}_2\text{O}$ /sodium ascorbate. ^g $[\text{Cu}(\text{MeCN})_4](\text{PF}_6)$. ^hIsolated yield.

3 ^1H and ^{13}C NMR Spectroscopy

HBC-alkyne-TIPS

^1H NMR (500 MHz, CDCl_3 , 298 K)

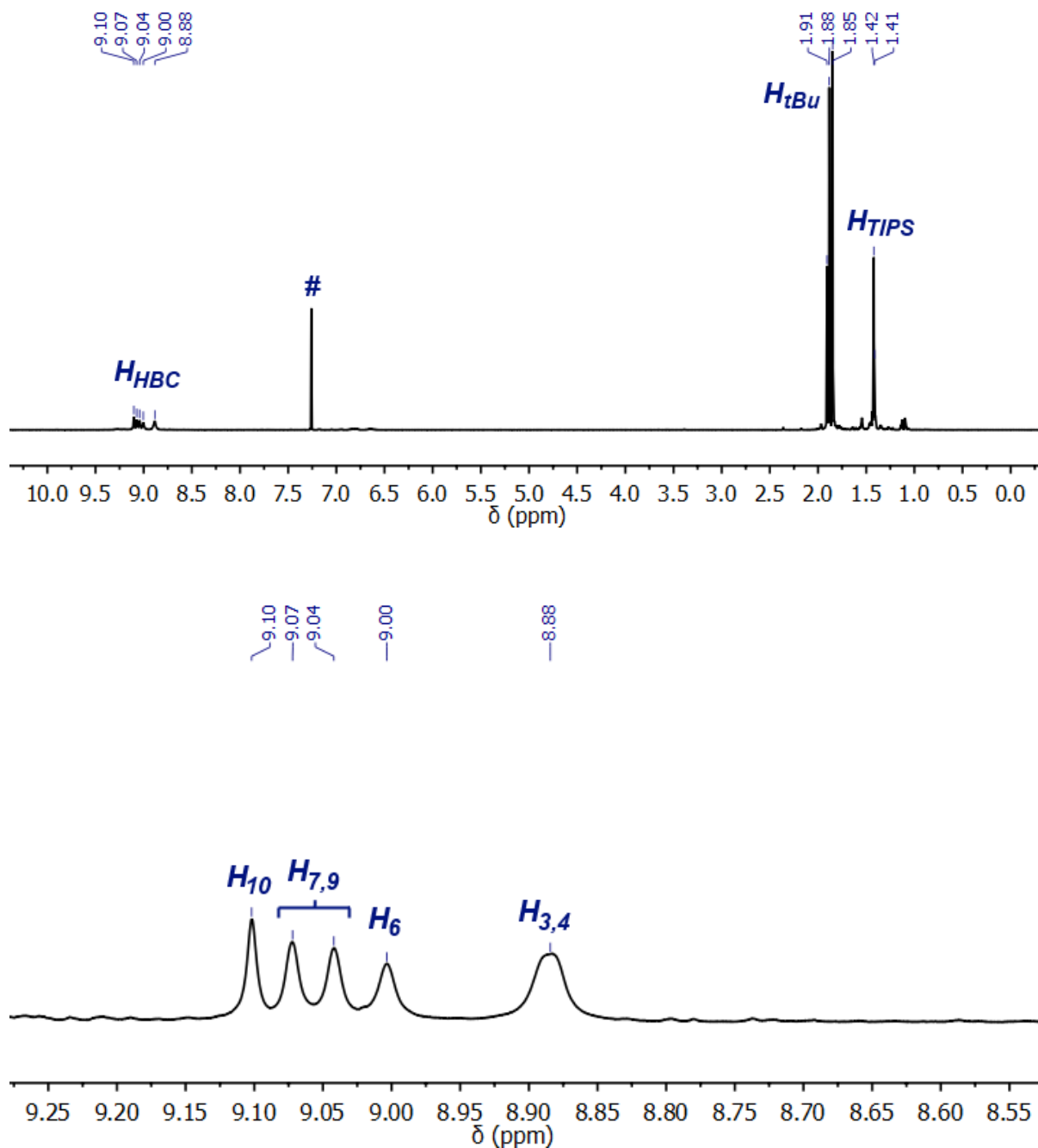


Figure 3.1 ^1H NMR spectrum of HBC-alkyne-TIPS displaying the full spectrum (above) and the aromatic region (9.2-8.6 ppm) below. $\# = \text{CHCl}_3$, $H_{\text{HBC}} = H_{3,4,6,7,9,10}$; $H_{\text{tBu}} = H_{45,47,53}$; $H_{\text{TIPS}} = H_{72,73}$.

^{13}C NMR (126 MHz, CDCl_3 , 298 K)

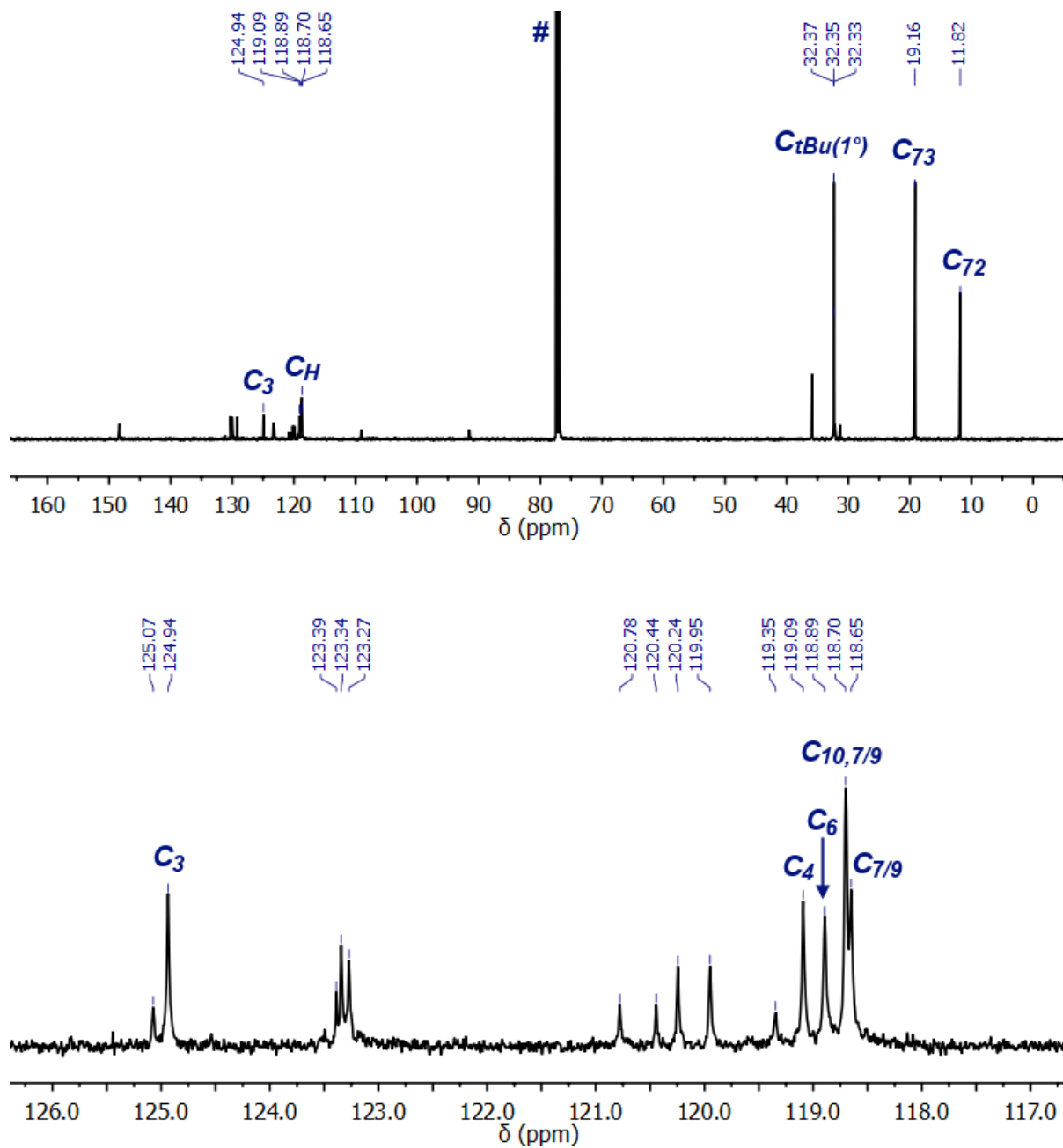


Figure 3.2 ^{13}C NMR spectrum of HBC-alkyne-TIPS displaying the full spectrum (above) and a section of the aromatic region (126-117 ppm) below. # = CDCl_3 solvent signal. Only signals of protonated carbon atoms are labelled; for full assignment, refer to experimental section (*vide infra*). $\text{C}_{\text{tBu}}(1^\circ) = \text{C}_{45,47,53}$, $\text{C}_\text{H} = \text{C}_{4,6,7,9,10}$.

1,2,3-Triazole 1a

^1H NMR (500 MHz, CDCl_3 , 298 K)

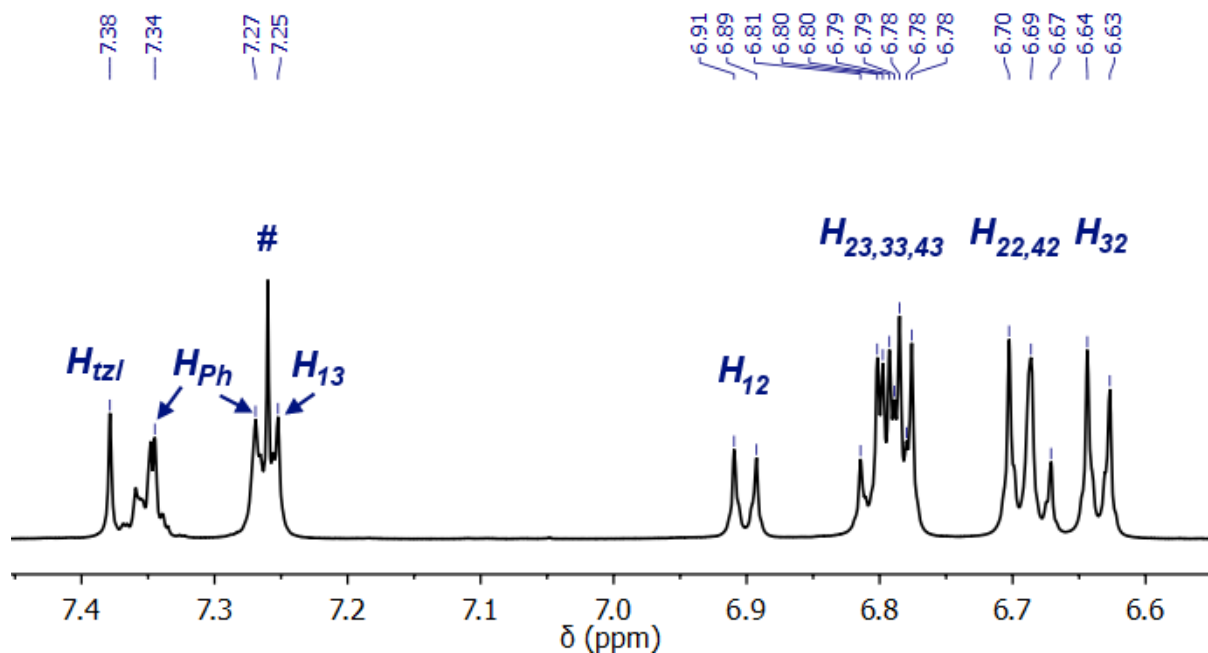
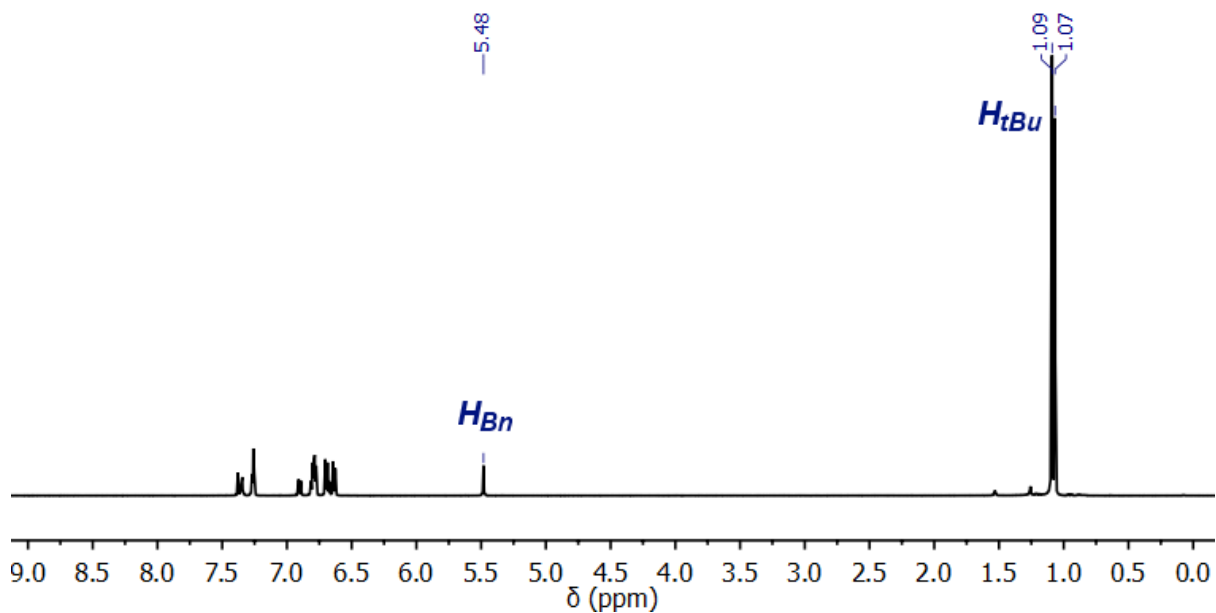


Figure 3.3 ^1H NMR spectrum of 1,2,3-triazole **1a** displaying the full spectrum (above) and the aromatic region (7.5-6.5 ppm) below. # = CHCl_3 . $H_{Ph} = H_{74,75,76}$; $H_{tzl} = H_{71}$.

^{13}C NMR (126 MHz, CDCl_3 , 298 K)

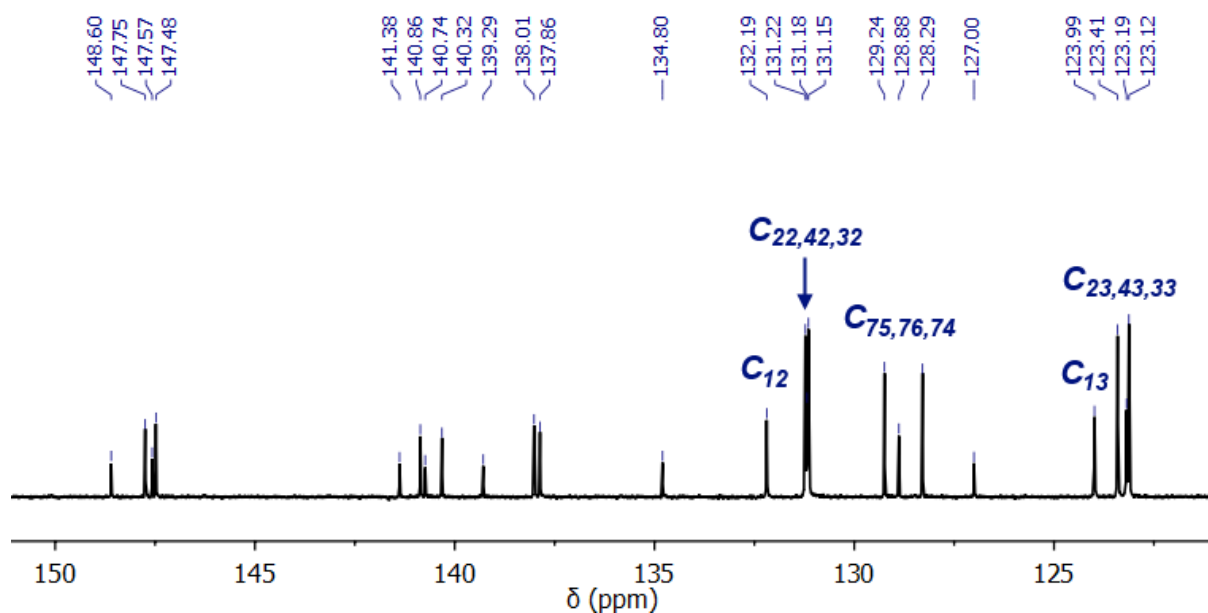
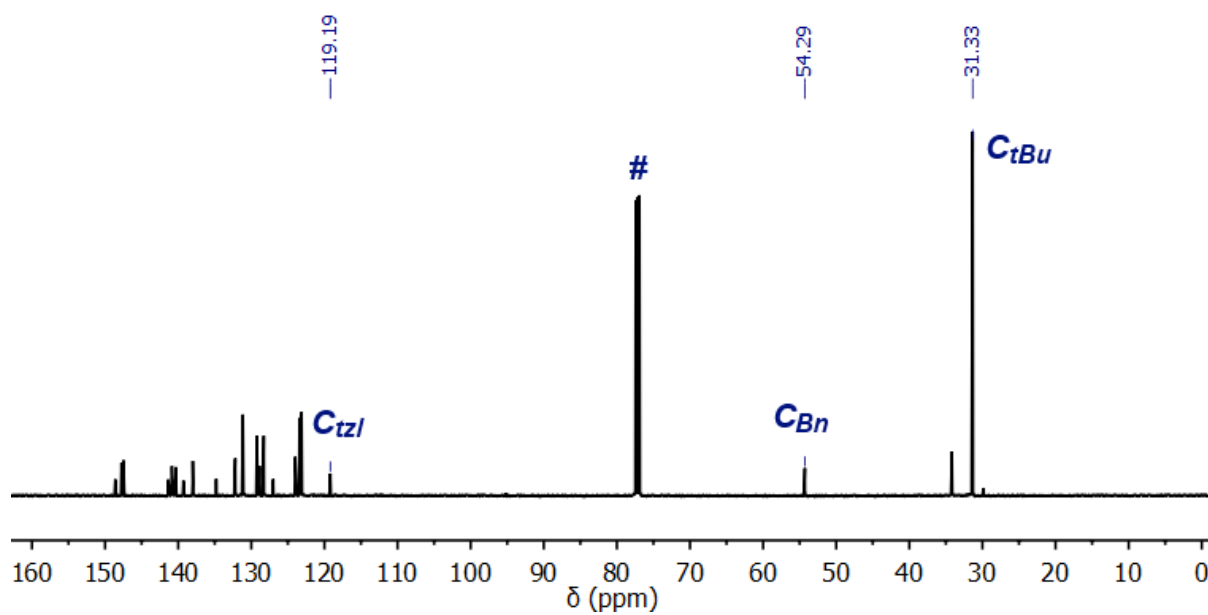


Figure 3.4 ^{13}C NMR spectrum of 1,2,3-triazole **1a** displaying the full spectrum (above) and the aromatic region (150-120 ppm) below. # = CDCl_3 solvent signal. Only signals of protonated carbon atoms are labelled; for full assignment, refer to experimental section (*vide infra*). C_{tBu} = $C_{28,38,48}$, C_{tZl} = C_{71} , C_{Bn} = C_{72} .

1,2,3-Triazole **1b**

^1H NMR (500 MHz, CDCl_3 , 298 K)

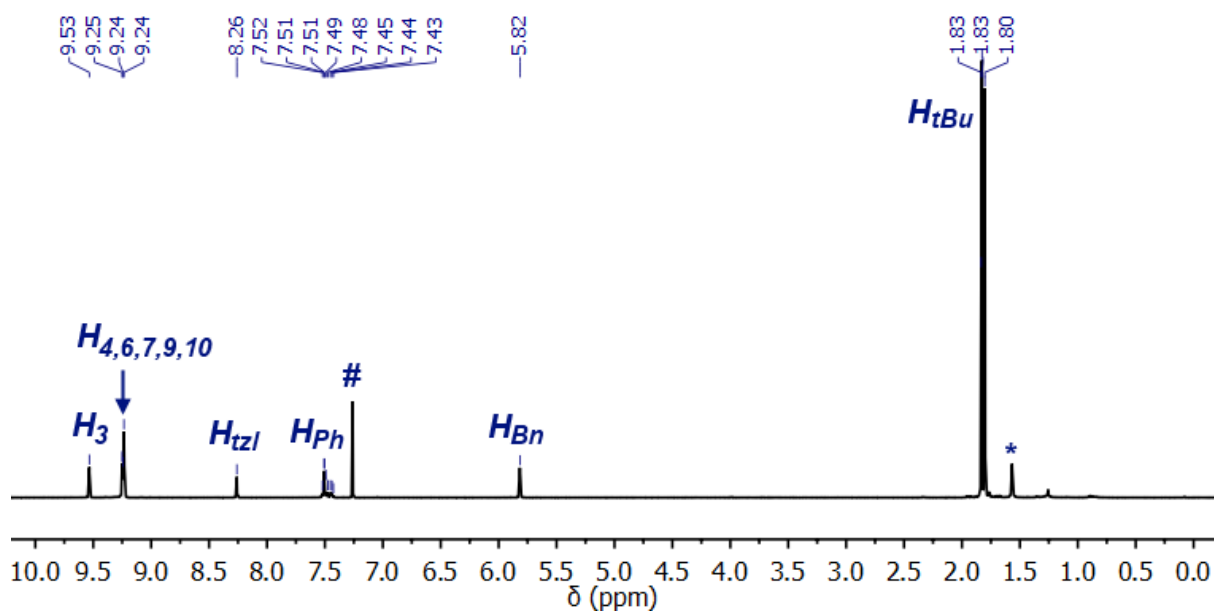


Figure 3.5 ^1H NMR spectrum of 1,2,3-triazole **1b** displaying the full spectrum. $\# = \text{CHCl}_3$, $*$ = H_2O . $H_{ph} = H_{74,75,76}$, $H_{tzl} = H_{71}$, $H_{Bn} = H_{72}$, $H_{tBu} = H_{45,49,53}$.

^{13}C NMR (126 MHz, CDCl_3 , 298 K)

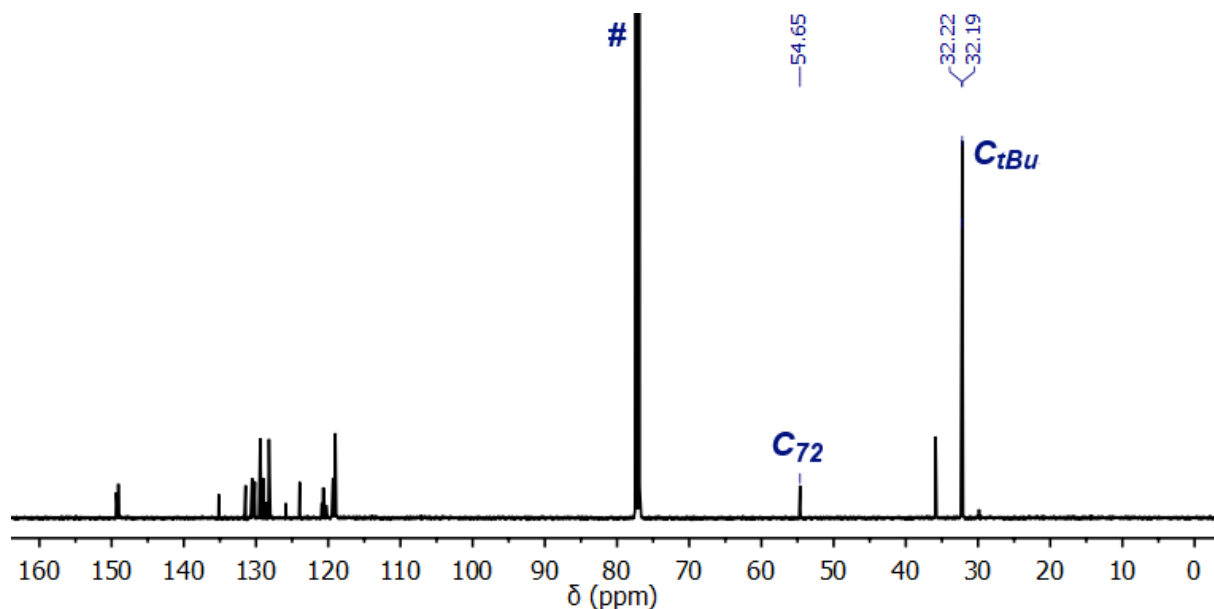


Figure 3.6 ^{13}C NMR spectrum of 1,2,3-triazole **1b** displaying the full spectrum. $\# = \text{CDCl}_3$. Only signals of protonated carbon atoms are labelled; for full assignment, refer to experimental section (*vide infra*). $C_{tBu} = C_{45,49,53}$.

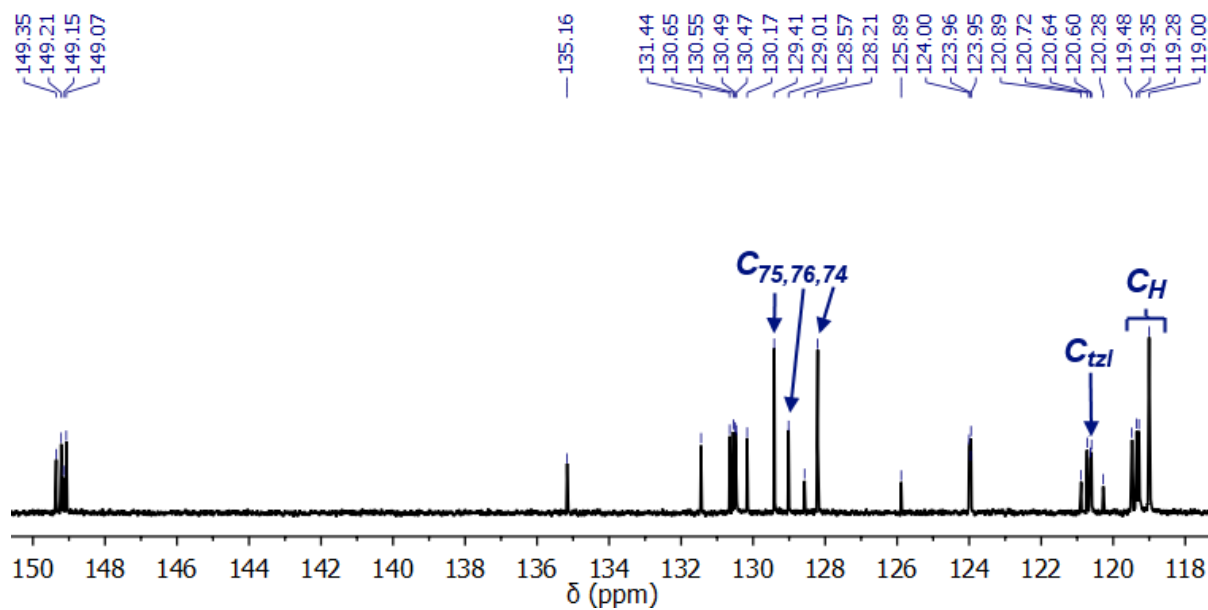


Figure 3.7 ^{13}C NMR spectrum of 1,2,3-triazole **1b** displaying the aromatic region (150-118 ppm). Only signals of protonated carbon atoms are labelled; for full assignment, refer to experimental section (*vide infra*). $C_H = C_{3,4,6,7,9,10}$. $C_{tzl} = C_{71}$.

Dichlorobis(triazole)palladium(II) Complex **2a**

^1H NMR (500 MHz, CDCl_3 , 298 K)

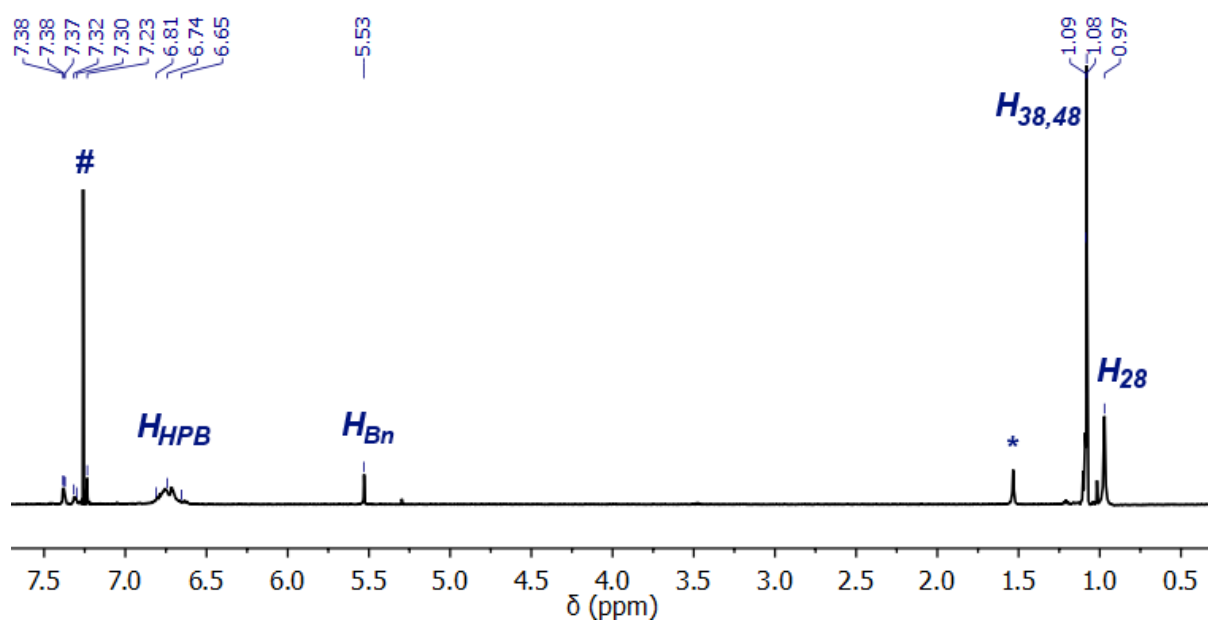


Figure 3.8 ^1H NMR spectrum of palladium complex **2a** displaying the full spectrum. # = CHCl_3 . * = H_2O . $H_{HPB} = H_{12,13,22,23,32,33,42,43}$, $H_{Bn} = H_{72}$.

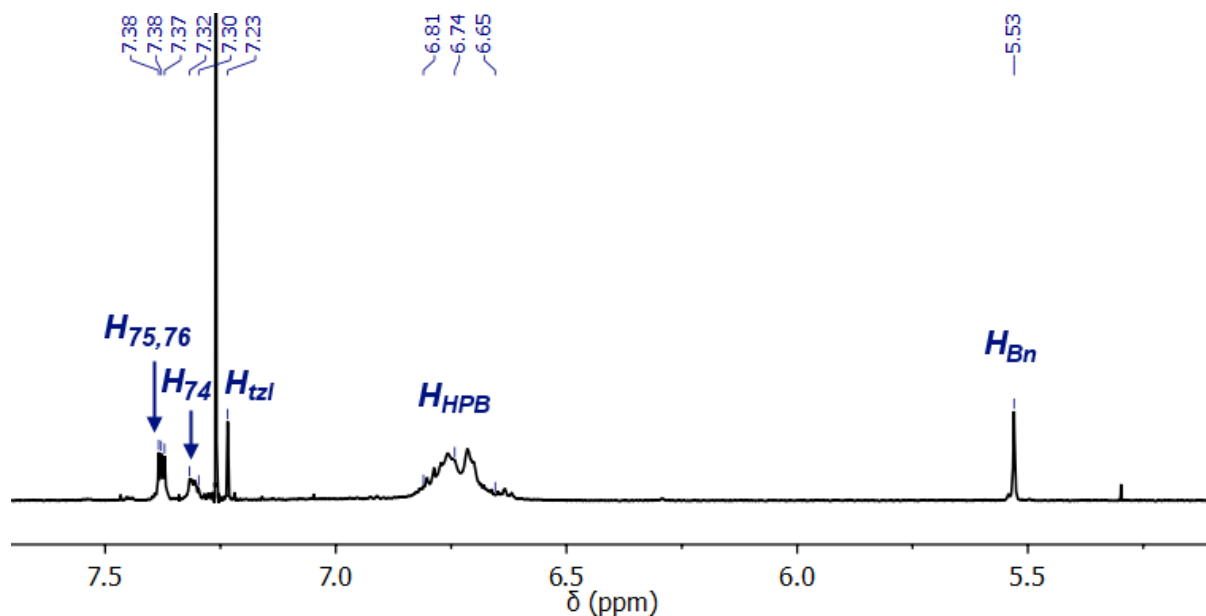


Figure 3.9 ^1H NMR spectrum of palladium complex **2a** displaying the aromatic region (5.0-7.5 ppm) spectrum. $\text{H}_{\text{HPB}} = \text{H}_{12,13,22,23,32,33,42,43}$, $\text{H}_{\text{Bn}} = \text{H}_{72}$, $\text{H}_{\text{tzl}} = \text{H}_{71}$.

^{13}C NMR (126 MHz, CDCl_3 , 298 K)

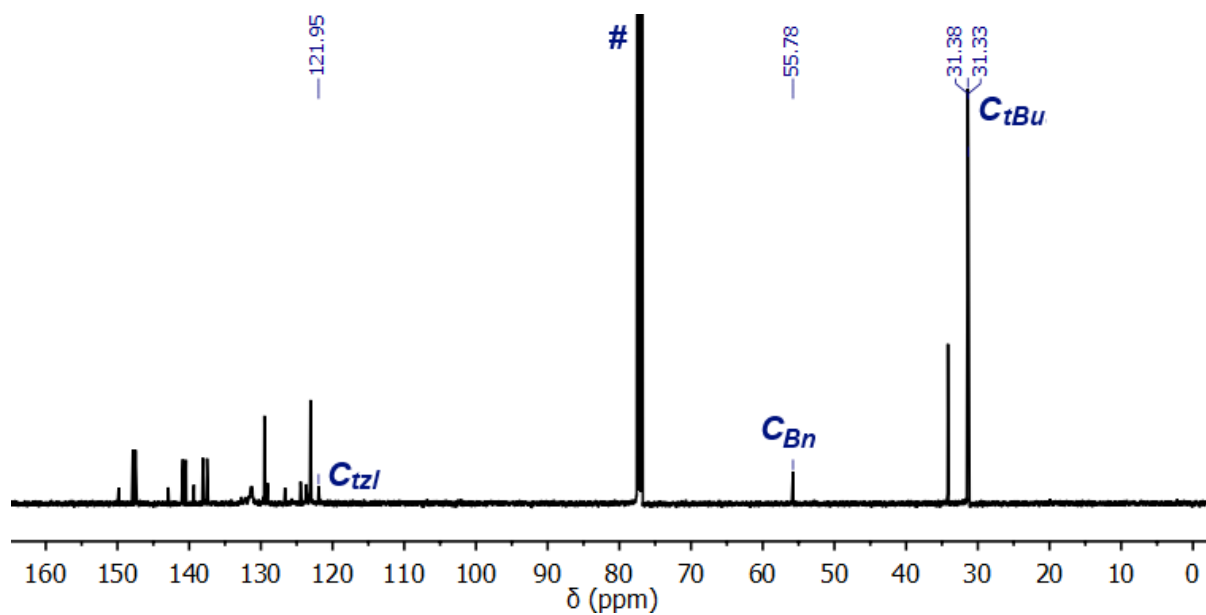


Figure 3.10 ^{13}C NMR spectrum of palladium complex **2a** displaying the full spectrum. # = CDCl_3 . $\text{C}_{\text{tBu}} = \text{C}_{28,38,48}$, $\text{C}_{\text{Bn}} = \text{C}_{72}$. $\text{C}_{\text{tzl}} = \text{C}_{71}$.

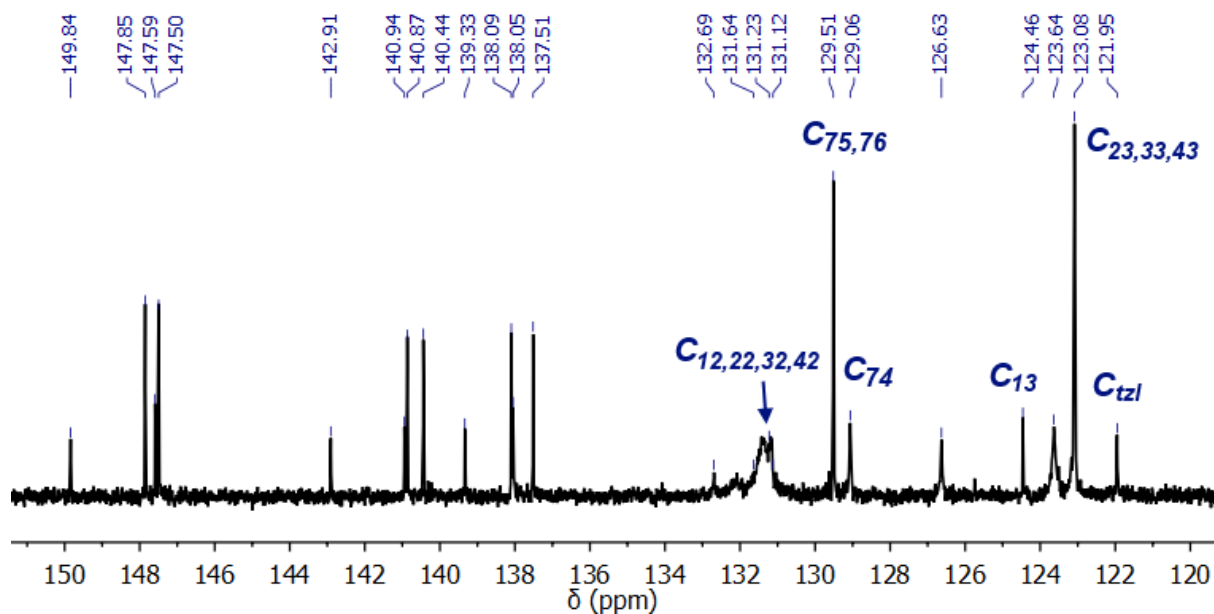


Figure 3.11 ^{13}C NMR spectrum of palladium complex **2a** displaying the aromatic region (150–120 ppm). Only signals of protonated carbon atoms are labelled; for full assignment, refer to experimental section (*vide infra*). $C_{\text{tzl}} = C_{71}$.

Dichlorobis(triazole)palladium(II) Complex **2b**

^1H NMR (500 MHz, CDCl_3 , 298 K)

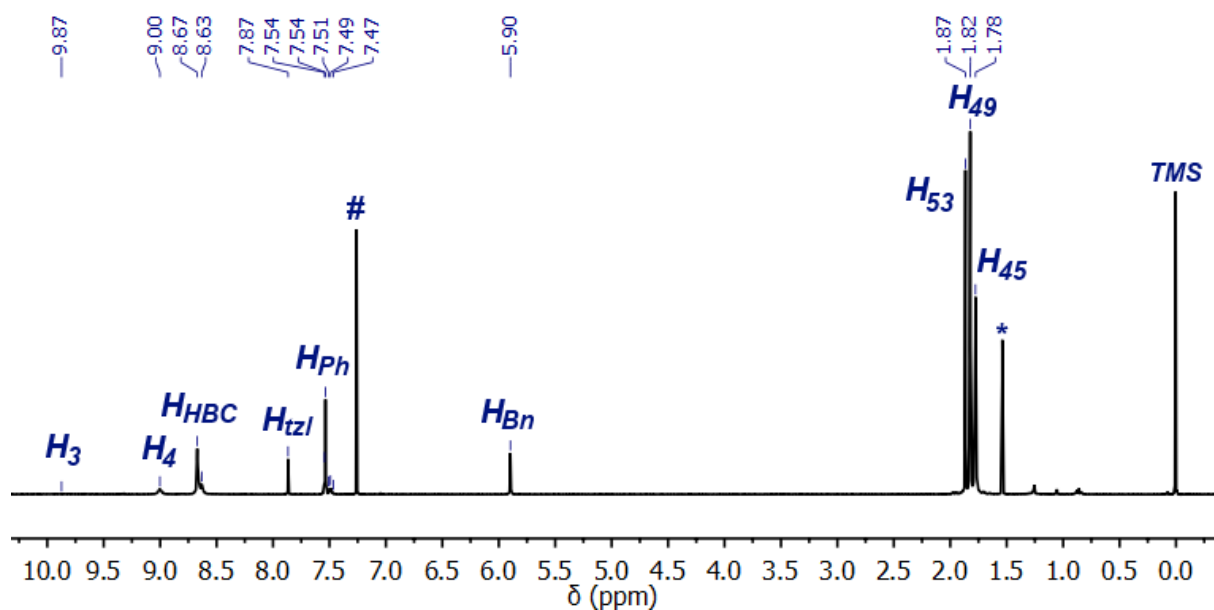


Figure 3.12 ^1H NMR spectrum of palladium complex **2b** displaying the full spectrum. # = CHCl_3 . * = H_2O . TMS = tetramethylsilane. $H_{\text{HBC}} = H_{6,7,9,10}$, $H_{\text{tzl}} = H_{71}$, $H_{\text{Ph}} = H_{74,75,76}$, $H_{\text{Bn}} = H_{72}$.

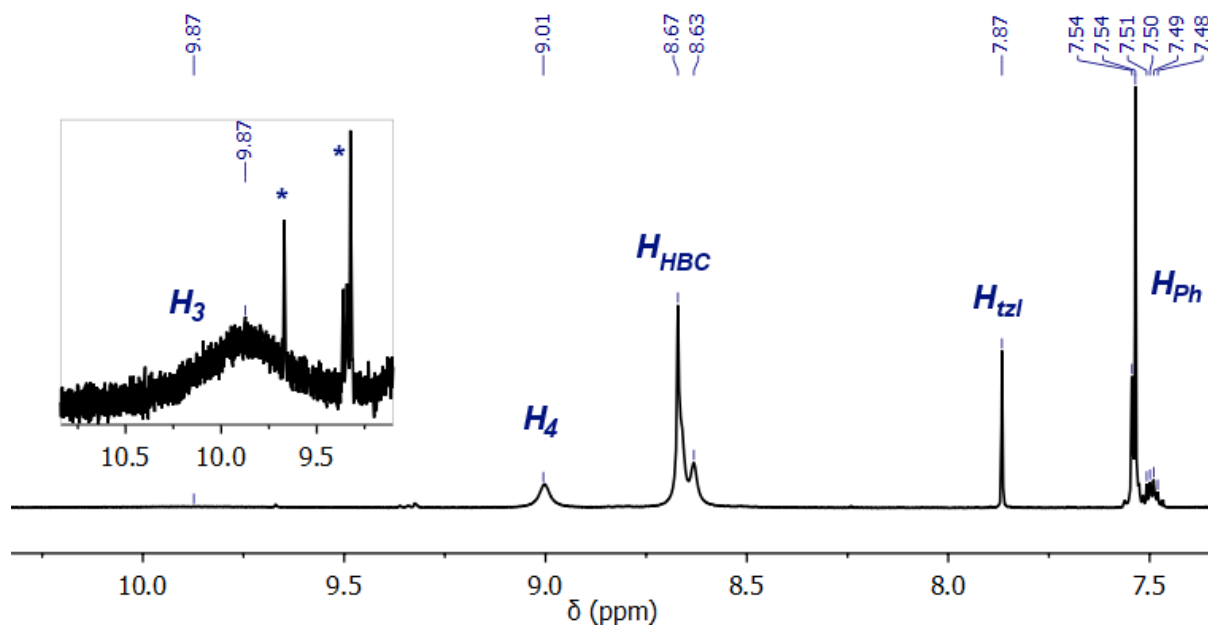


Figure 3.13 ^1H NMR spectrum of palladium complex **2b** displaying the aromatic region (10.5-7.4 ppm). * = ligand **1b** impurity. $H_{\text{HBC}} = H_{6,7,9,10}$, $H_{\text{tzt}} = H_{71}$, $H_{\text{Ph}} = H_{74,75,76}$.

^{13}C NMR (126 MHz, CDCl_3 , 298 K)

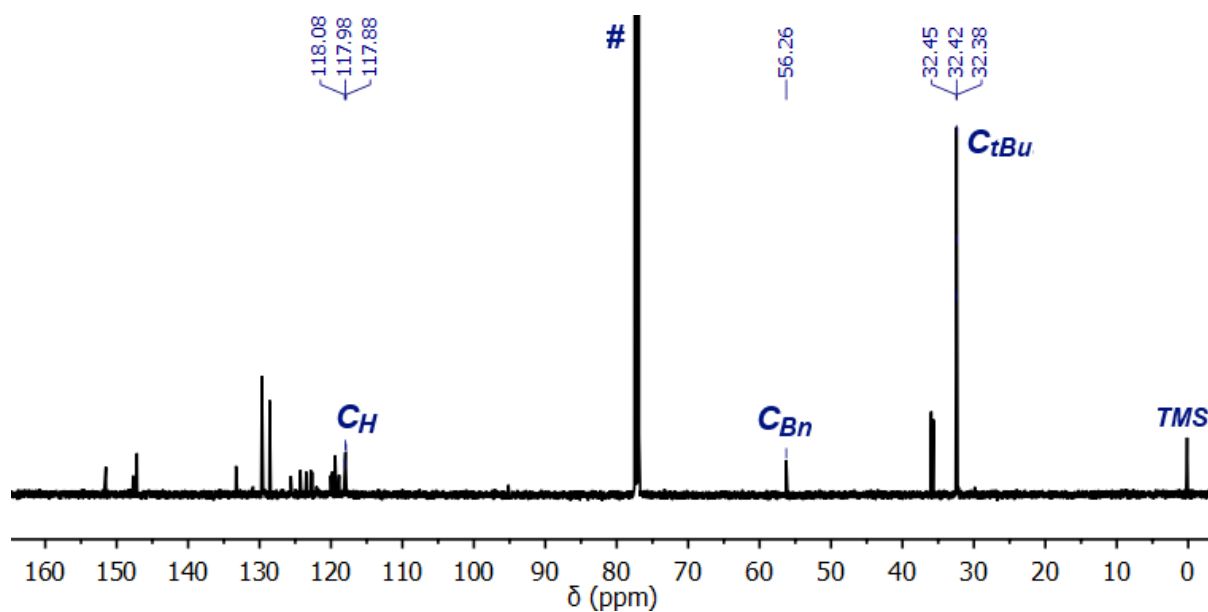


Figure 3.14 ^{13}C NMR spectrum of palladium complex **2b** displaying the full spectrum. # = CDCl_3 . TMS = tetramethylsilane. $C_{\text{tBu}} = C_{45,49,53}$, $C_{\text{Bn}} = C_{72}$, $C_{\text{H}} = C_{3,4,6,7,9,10}$.

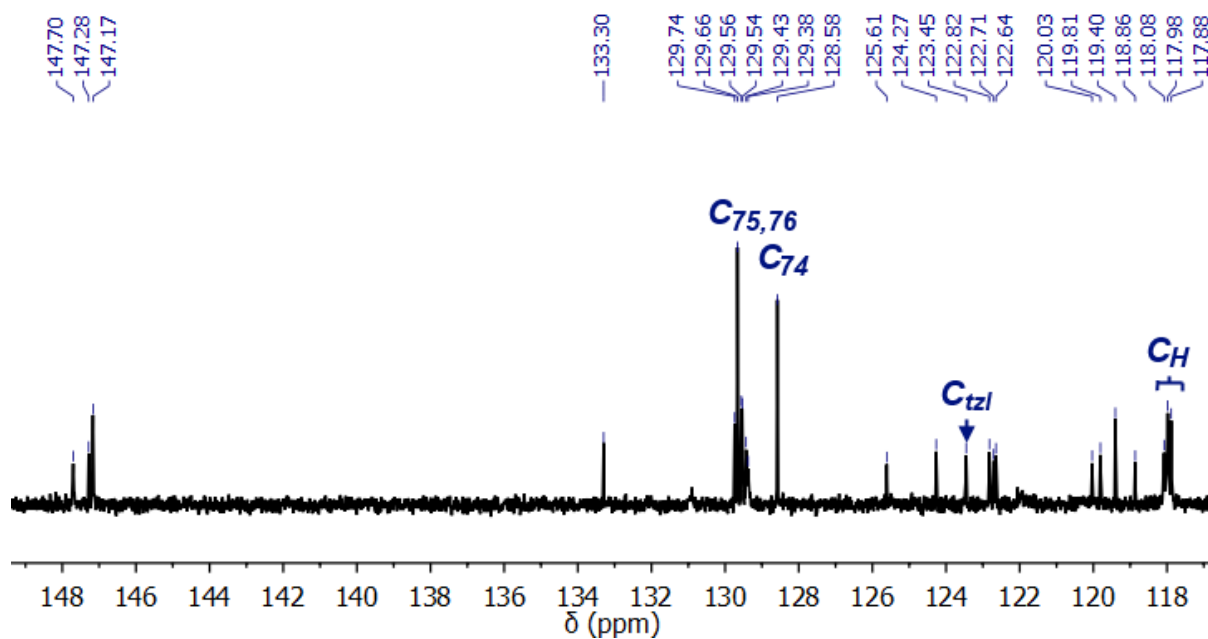


Figure 3.15 ^{13}C NMR spectrum of palladium complex **2b** displaying the aromatic region (150-117 ppm). Only signals with protonated carbon atoms are labelled; for full assignment, refer to experimental section (*vide infra*). $C_H = C_{3,4,6,7,9,10}$. $C_{tzl} = C_{71}$.

Dibromo(benzimidazolylidene)(triazole)palladium(II) Probe Complex 4a

^1H NMR (400 MHz, CDCl_3 , 298 K)

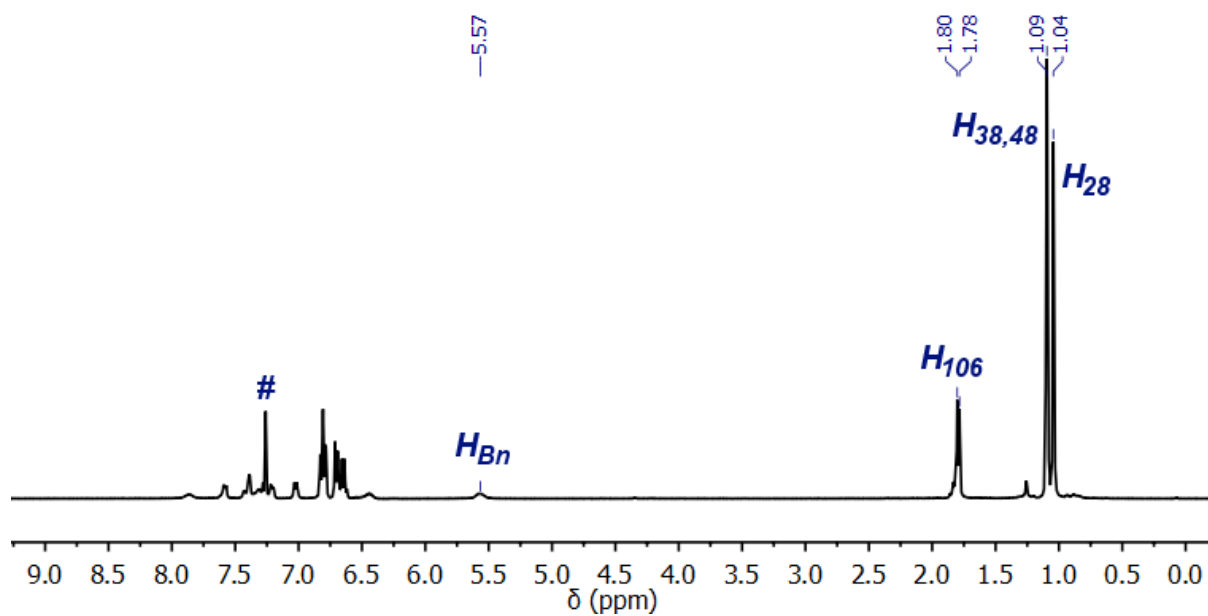


Figure 3.16 The full ^1H NMR spectrum of palladium complex **4a**. # = CHCl_3 . $H_{Bn} = H_{72}$.

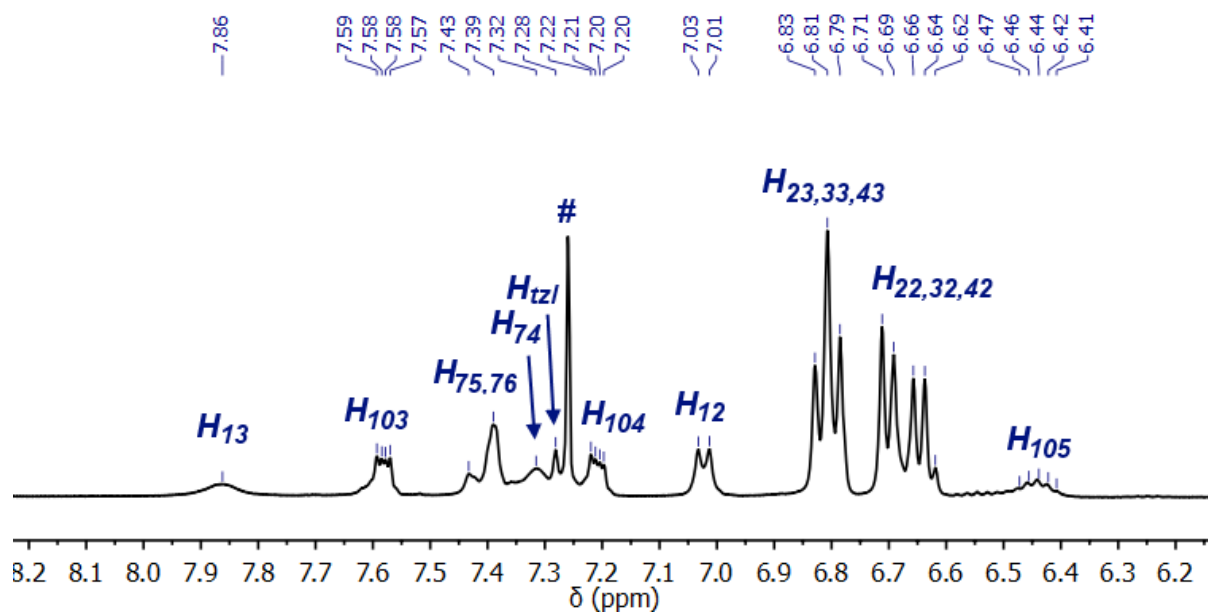


Figure 3.17 The ^1H NMR spectrum of the aromatic region of palladium complex **4a**. # = CHCl_3 . $H_{tzi} = H_{71}$.

^{13}C NMR (126 MHz, CDCl_3 , 298 K)

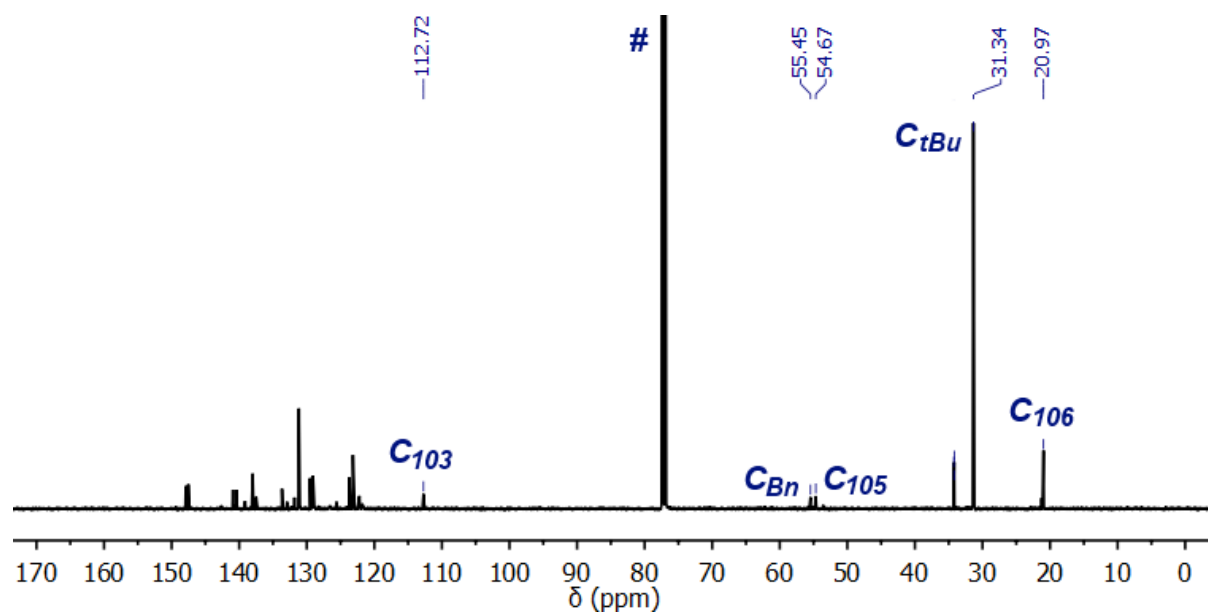


Figure 3.18 The full ^{13}C NMR spectrum of palladium complex **4a**. # = CDCl_3 . $C_{tBu} = C_{28,38,48}$, $C_{Bn} = C_{72}$. The carbene signal (C_{101}) was not observed.

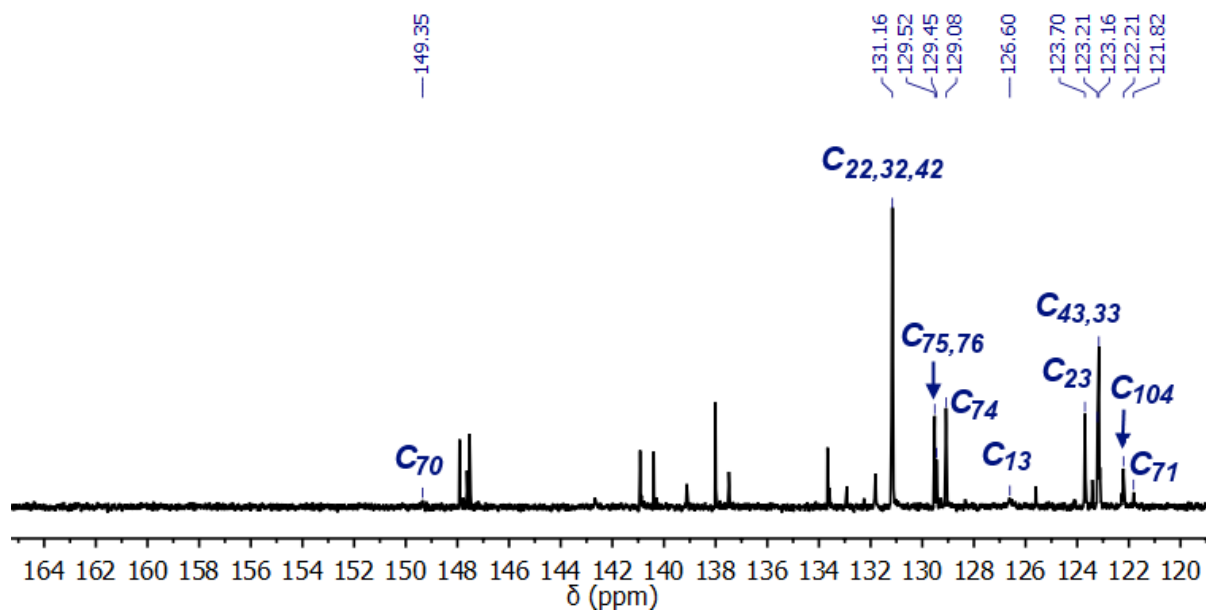


Figure 3.19 The ^{13}C NMR spectrum of the aromatic region of palladium complex **4a**. The carbene signal (C_{101}) was not observed. With the exception of C_1 all labelled signals correspond to protonated carbon atoms.

Dibromo(benzimidazolylidene)(triazole)palladium(II) Probe Complex **4b**

^1H NMR (400 MHz, CDCl_3 , 298 K)

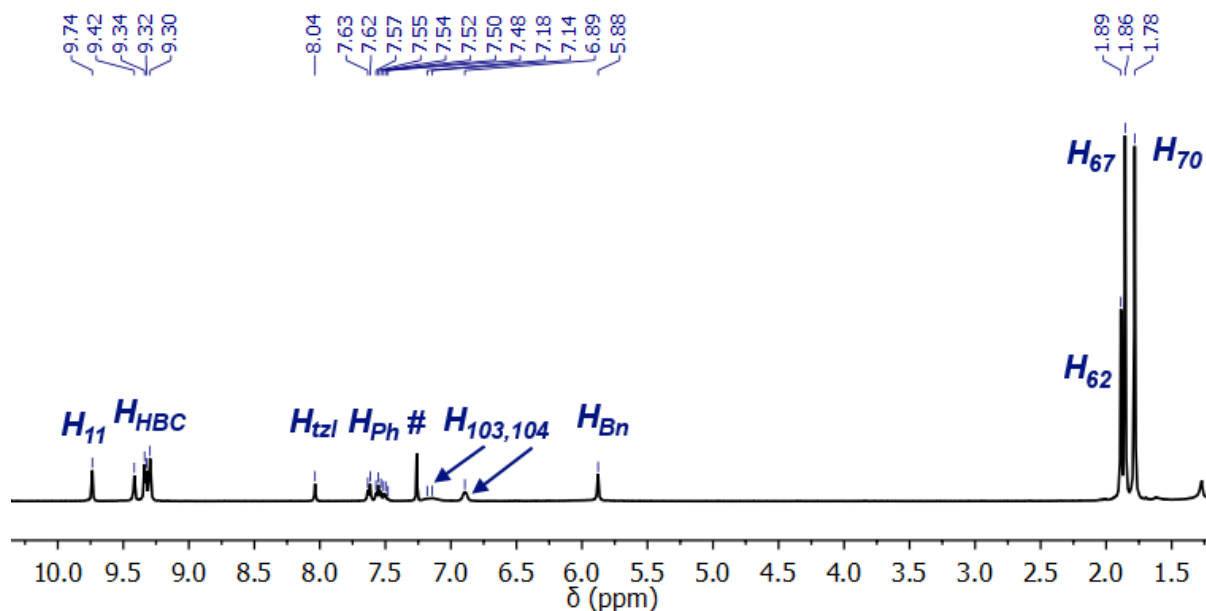


Figure 3.20 ^1H NMR spectrum of palladium complex **4b** displaying the full spectrum. # = CHCl_3 solvent impurity. H_{HBC} = $H_{4,6,7,9,10}$, H_{tzl} = H_{71} , H_{Ph} = $H_{74,75,76}$, H_{Bn} = H_{72} .

^{13}C NMR (126 MHz, CDCl_3 , 298 K)

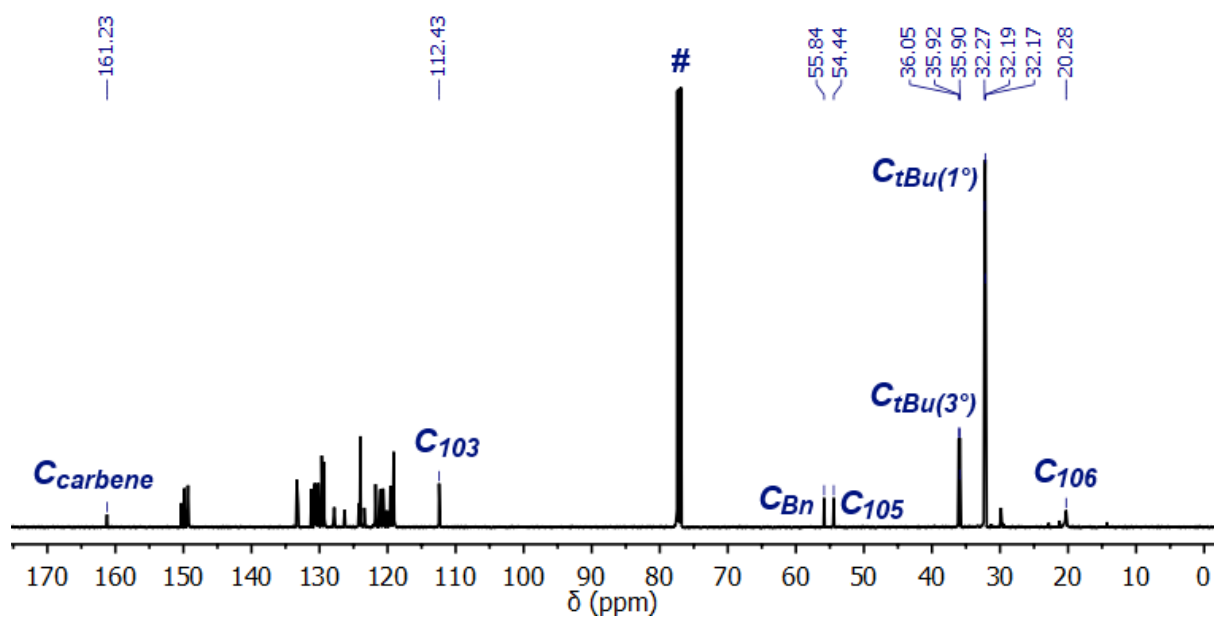


Figure 3.21 The full ^{13}C NMR spectrum of palladium complex **4b**. $\# = \text{CDCl}_3$. $\text{C}_{\text{tBu}(1^\circ)} = \text{C}_{45,49,53}$, $\text{C}_{\text{tBu}(3^\circ)} = \text{C}_{44,48,52}$, $\text{C}_{\text{Bn}} = \text{C}_{72}$, $\text{C}_{\text{carbene}} = \text{C}_{101}$.

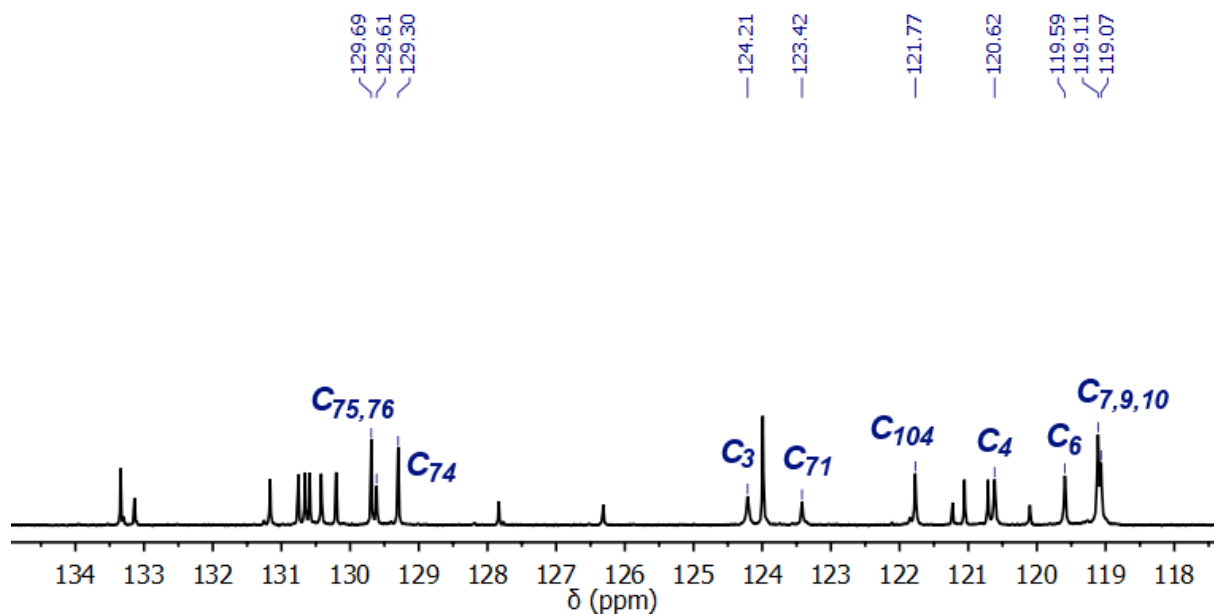


Figure 3.22 ^{13}C NMR spectrum of palladium complex **4b** displaying the signals of protonated carbon atoms (labelled) of the aromatic region (134-118 ppm).

¹H NMR Stackplots

Formation of Complex 2a

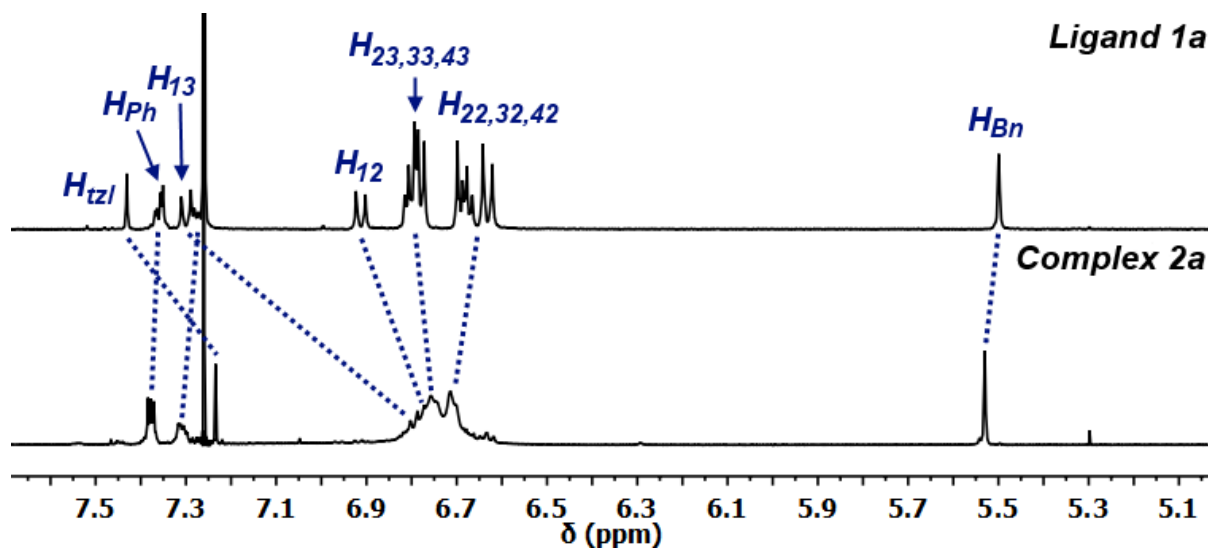


Figure 3.23 Stacked ¹H NMR spectra of ligand **1a** and subsequent PdCl₂L₂ complex **2a**, displaying chemical shift changes upon complexation.

Formation of Complex 2b

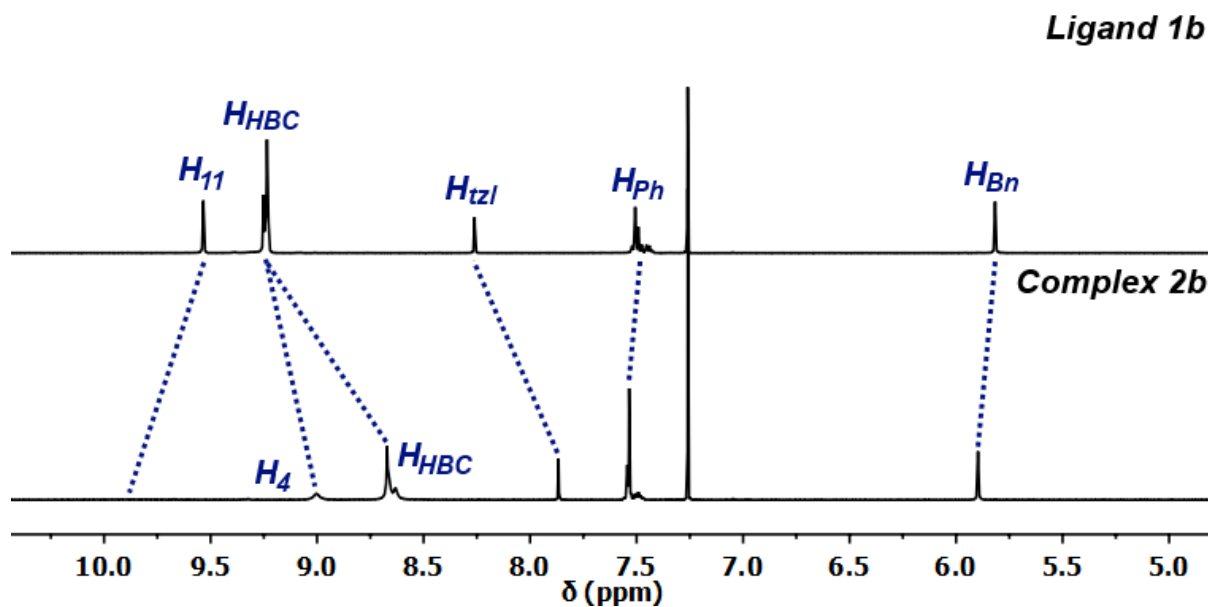


Figure 3.24 Stacked ¹H NMR spectra of ligand **1b** and subsequent PdCl₂L₂ complex **2b**, displaying chemical shift changes upon complexation.

Formation of Complex 4a

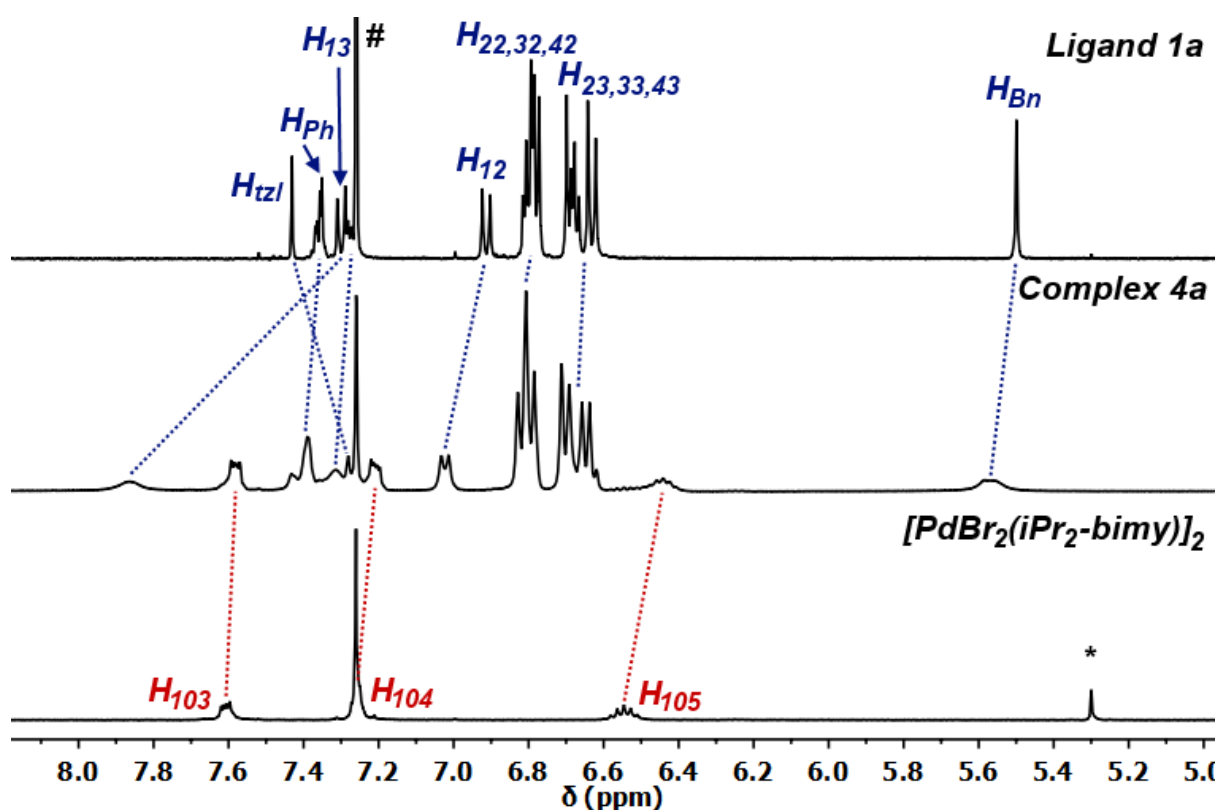


Figure 3.25 Stacked ^1H NMR spectra of ligand 1a and precursor $[\text{PdBr}_2(\text{iPr}_2\text{-bimy})]_2$ to form Pd probe complex 4a, displaying the changes in chemical shift upon complexation. # = CHCl_3 . * CH_2Cl_2 .

Formation of Complex 4b

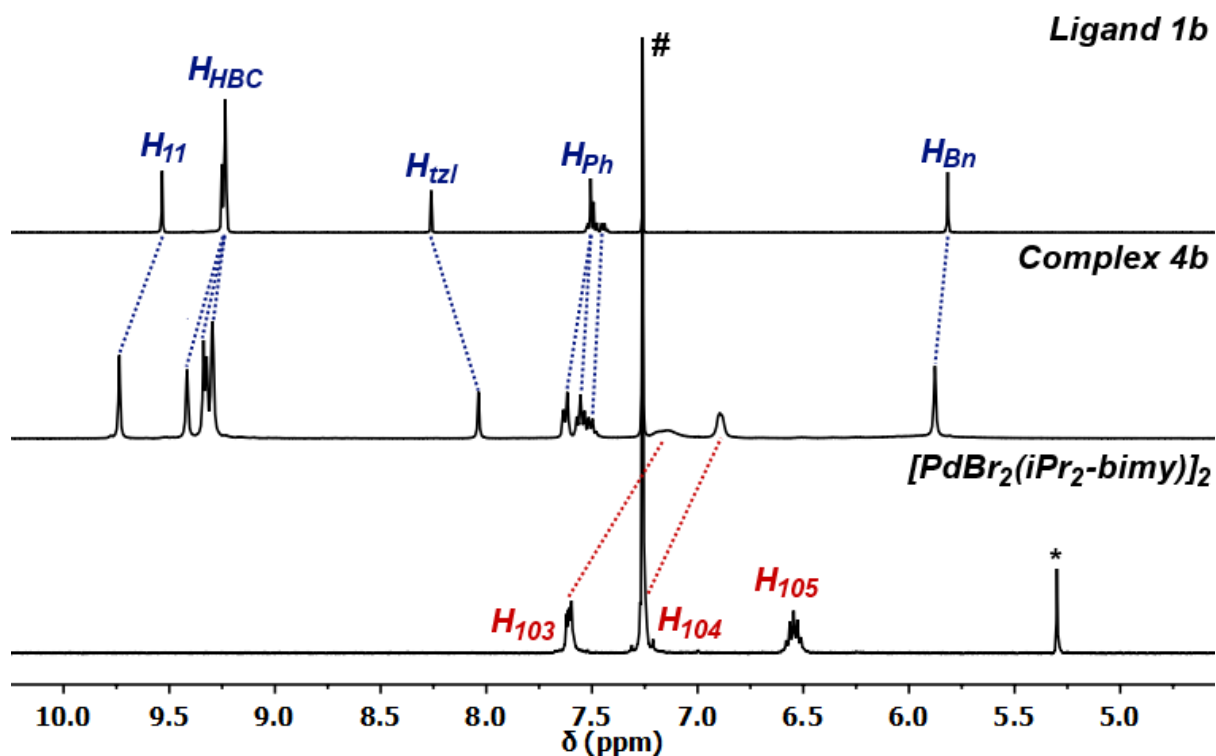


Figure 3.26 Stacked ^1H NMR spectra of ligand 1b and precursor $[\text{PdBr}_2(\text{iPr}_2\text{-bimy})]_2$ to form Pd probe complex 4b, displaying the changes in chemical shift upon complexation. # = CHCl_3 . * CH_2Cl_2 .

4 MALDI-TOF Mass Spectrometry

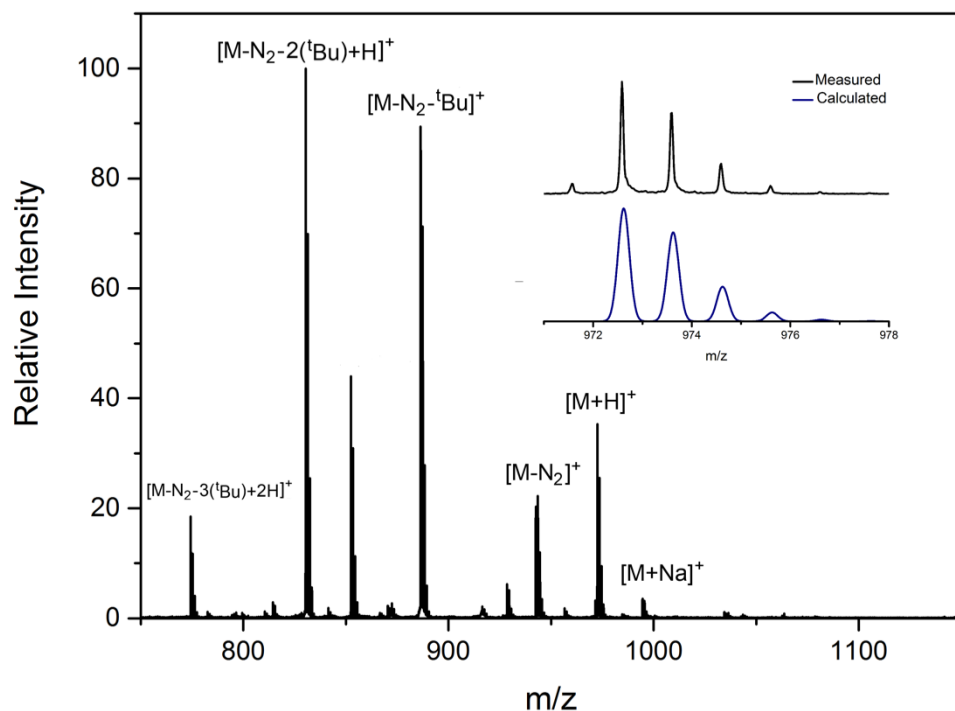


Figure 4.1 MALDI-TOF-MS of HPB triazole **1a**. The inset displays the measured and calculated isotope profiles of the $[M+H]^+$ peak.

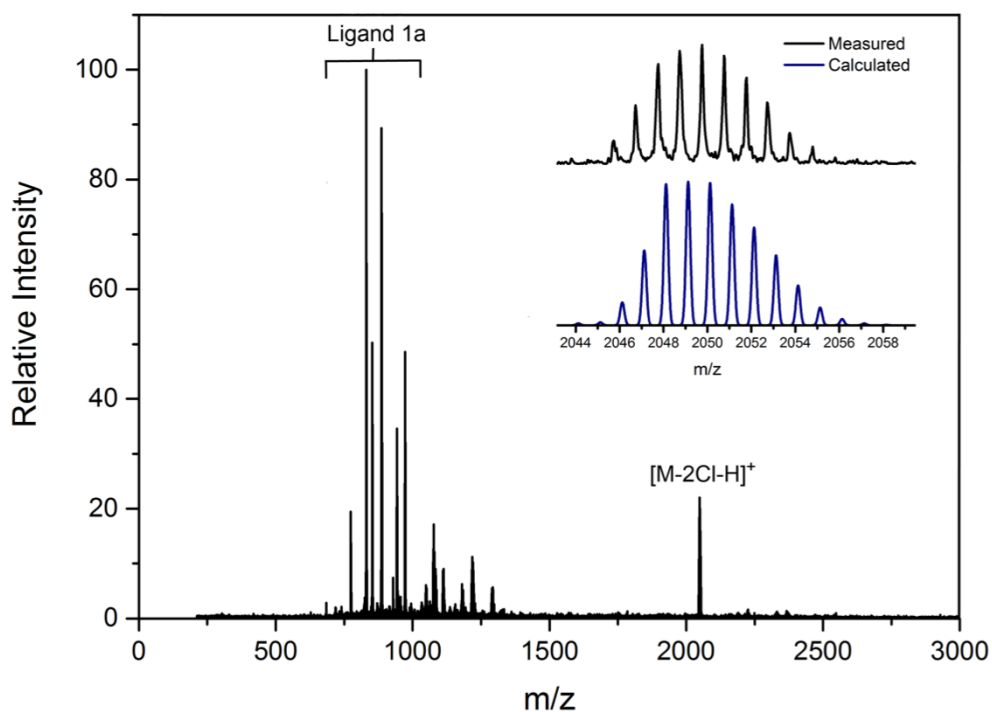


Figure 4.2 MALDI-TOF-MS of palladium complex **2a**. The inset displays the measured and calculated isotope profiles of $[M-2Cl-H]^+$ peak.

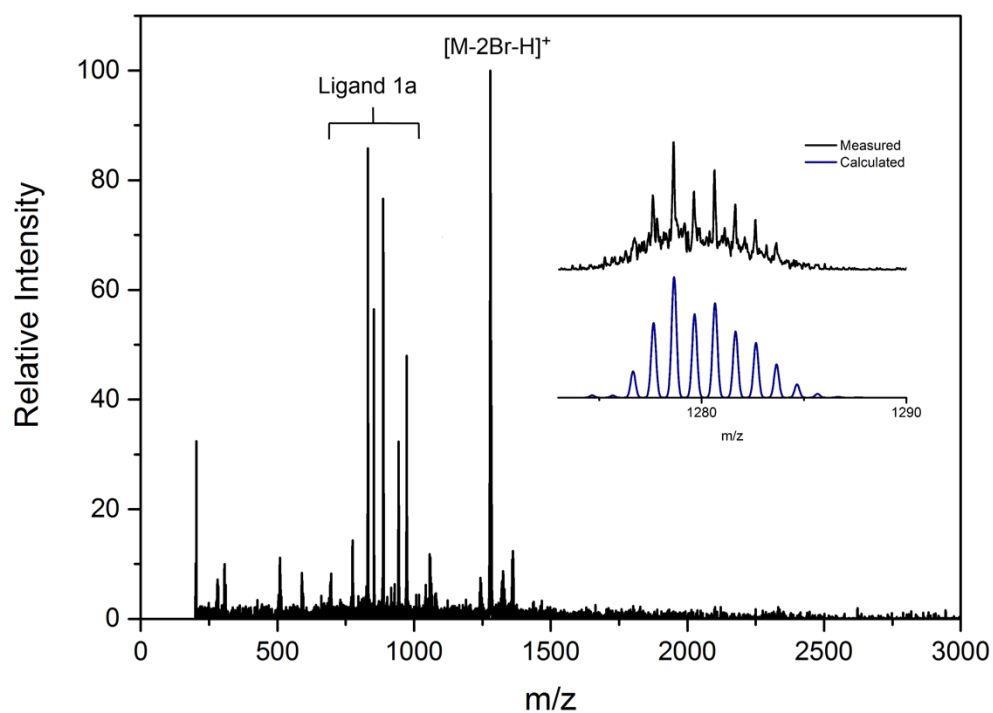


Figure 4.3 MALDI-TOF-MS of palladium probe complex **4a**. The inset displays the measured and calculated isotope profiles of $[M-2Br-H]^+$ peak.

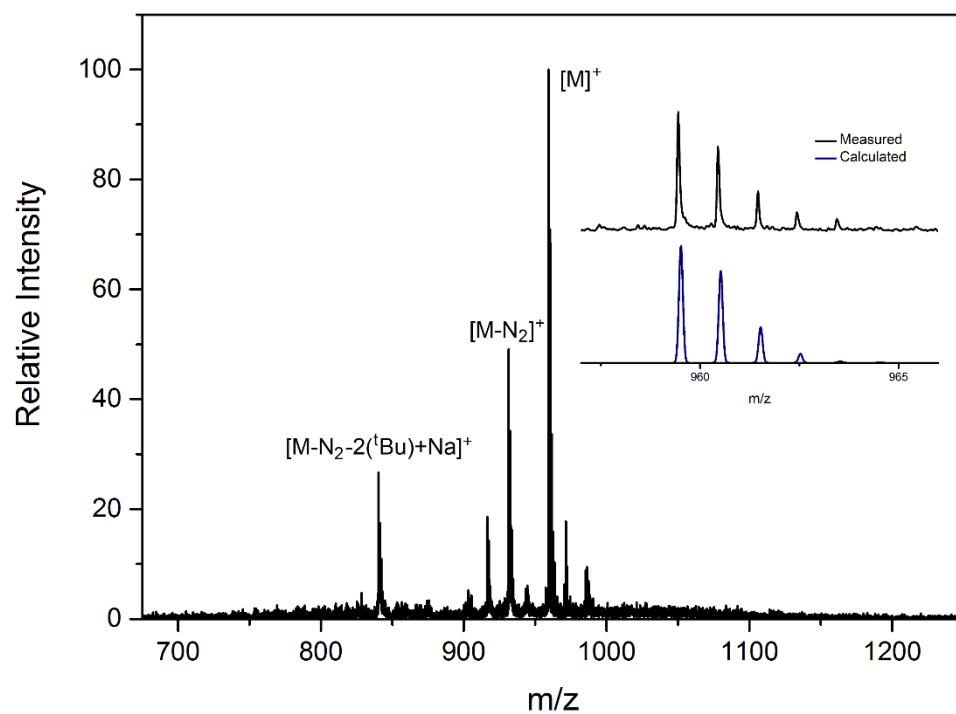


Figure 4.4 MALDI-TOF-MS of HBC triazole **1b**. The inset displays the measured and calculated isotope profiles of the $[M]^+$ peak.

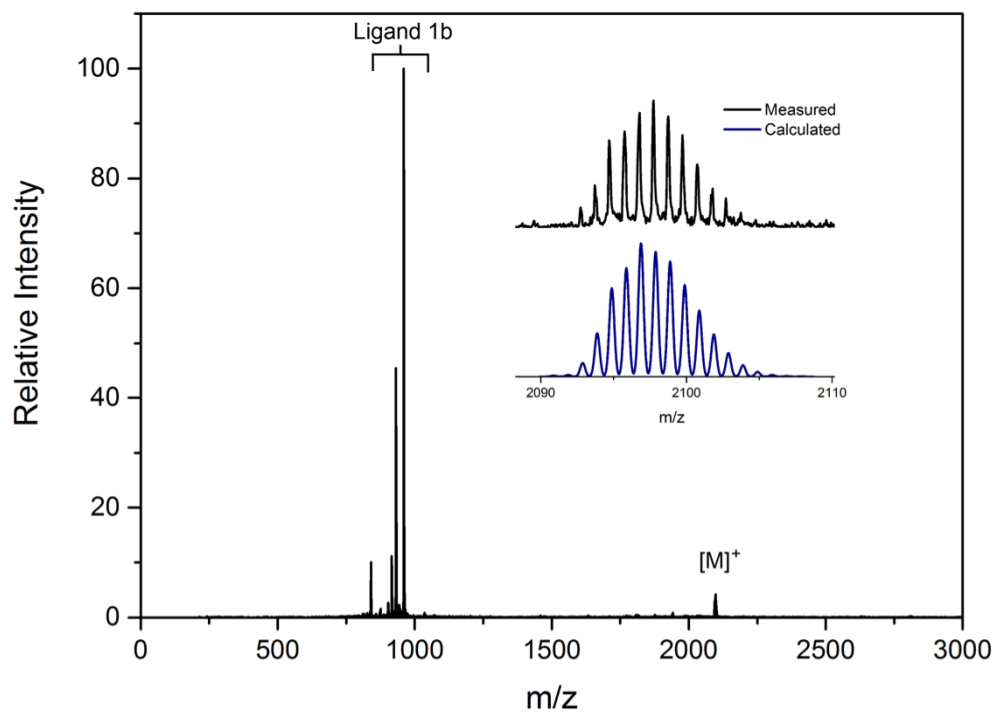


Figure 4.5 MALDI-TOF-MS of palladium(II) complex **2b**. The inset displays the measured and calculated isotope profiles of the $[M]^+$ peak.

5 Ligand Donor Strength

Synthesis

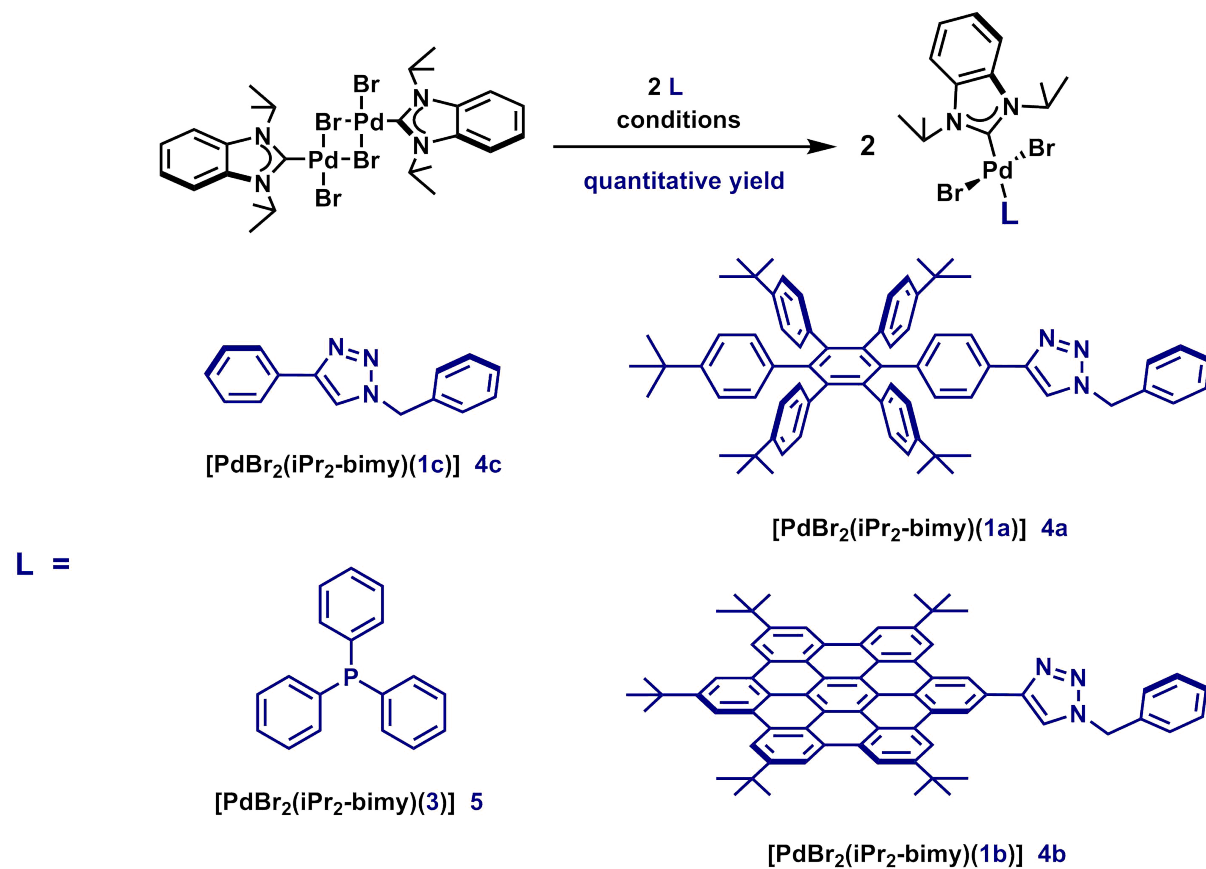


Figure 5.1 Synthesis of probe complexes **4a**, **4b**, **4c**, **5**.^{9, 10} Conditions: **4a**, **4b**: Ligand **4** (2.0 eq.), [PdBr₂(iPr₂-bimy)]₂ (1.0 eq.) CHCl₃, reflux, 4 h, quantitative.

Superimposed ¹³C NMR Spectra of Reporter Carbene Complexes

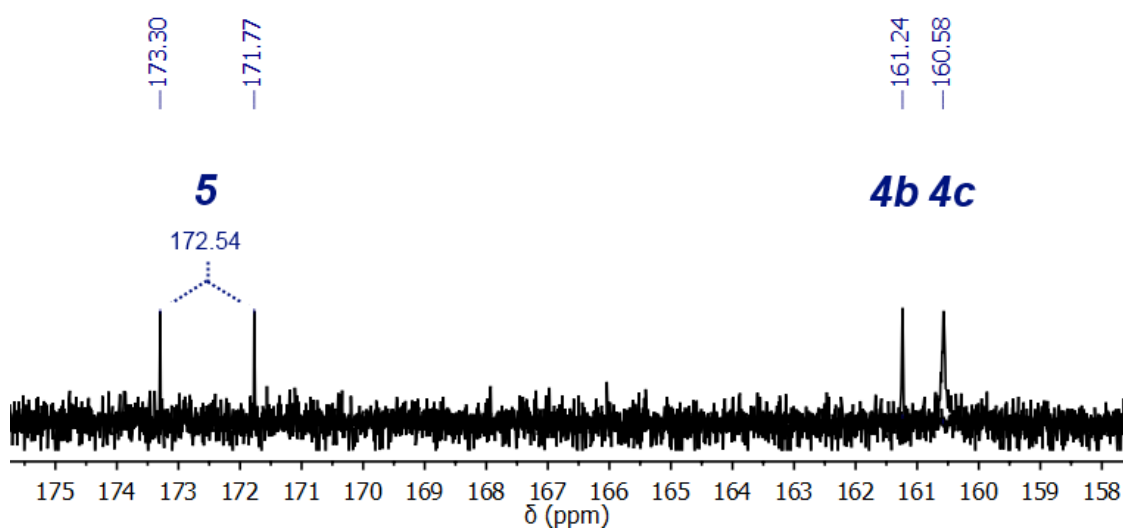


Figure 5.2 Superimposed ¹³C NMR spectra exhibiting the donor strengths of HBC-triazole based ligand **4b**, phenyl-triazole based **4c** and phosphine-based **3**.

6 X-ray Crystallography Data

General

Data were collected on an Agilent SuperNova with Atlas CCD using mirror monochromated microfocus Cu K α radiation ($\lambda = 1.54184 \text{ \AA}$) at 40 W. The data processing was undertaken within CrysAlisPro,¹¹ including a numerical absorption correction over a face-indexed model and/or a multiscan empirical correction. The structures were solved by direct methods with SHELXS-97¹² and extended and refined against all F^2 data with SHELXL-97¹² using the X-Seed interface.¹³ The non-hydrogen atoms in the asymmetric unit were modeled with anisotropic displacement parameters. Hydrogen atoms were placed in calculated positions and refined using a riding model with fixed C–H distances (sp^2 CH 0.95 \AA , sp^3 CH₃ 0.98 \AA , sp^3 CH₂ 0.99 \AA) and isotropic displacement parameters estimated as $U_{\text{iso}}(\text{H}) = 1.2U_{\text{eq}}(\text{C})$, except for CH₃, where $U_{\text{iso}}(\text{H}) = 1.5U_{\text{eq}}(\text{C})$.

The complexes **2b** and **4b** were refined using the SQUEEZE program in the PLATON package to account for highly disordered solvent regions.

Within the crystal of **2b**, there are two regions of disordered solvent of equal size per unit cell. The contents of each region which could not be effectively modelled were treated as a diffuse contribution to the overall scattering (total: 341 electrons, 2303 \AA^3). The electron count and volume are consistent with four acetonitrile and eight water molecules per void, with an electron count of 168 and volume of 1096 \AA^3 per void.

Within the crystal of probe complex **4b**, there is one region of disordered solvent per unit cell. The contents of the region could not be effectively modelled and was treated as a diffuse contribution to the overall scattering (total: 398 electrons, 1692 \AA^3). The electron count and volume fit consistently with 22 methanol molecules, with an electron count of 396 and volume of 1540 \AA^3 per void.

Crystal Data

	<i>trans-2a</i> ·7CH ₂ Cl ₂	<i>trans-2b</i>	<i>trans-4b</i>
CCDC No.	1502527	1502528	1502529
Crystallisation Solvents	CH ₂ Cl ₂ /MeOH	CH ₂ Cl ₂	CH ₂ Cl ₂ /MeOH
Empirical formula	C ₁₄₂ H ₁₅₄ Cl ₂ N ₆ Pd·7CH ₂ Cl ₂	C ₁₄₂ H ₁₃₀ Cl ₂ N ₆ Pd	C ₁₆₈ H ₁₆₆ Br ₄ N ₁₀ Pd ₂
Formula weight	2716.49	2097.82	2857.55
T(K)	100(2)	100.00(19)	100(2)
Crystal system	Triclinic	Monoclinic	Triclinic
Space group	<i>P</i> $\bar{1}$	<i>P</i> 2 ₁ / <i>c</i>	<i>P</i> $\bar{1}$
<i>a</i> (Å)	12.4144(3)	22.0530(6)	14.6518(2)
<i>b</i> (Å)	17.9604(4)	39.391(3)	16.6609(2)
<i>c</i> (Å)	33.3206(6)	14.3467(6)	33.4649(4)
α (°)	97.426(2)	90	97.6040(10)
β (°)	96.076(2)	99.711(3)	92.4960(10)
γ (°)	105.190(2)	90	92.4870(10)
<i>V</i> (Å ³)	7033.5(3)	12284.2(10)	8079.70(18)
<i>Z</i>	2	4	2
ρ_{calc} (mg mm ⁻³)	1.283	1.134	1.175
μ (mm ⁻¹)	4.253	2.004	3.330
Crystal size (mm)	0.32 x 0.14 x 0.04	0.21 x 0.06 x 0.03	0.29 x 0.14 x 0.07
Reflections collected	64885	51510	90409
Independent reflections (<i>R</i> _{int})	27763 (0.0603)	24388 (0.1036)	32171 (0.0334)
Data / restraints / parameters	27763/0/1579	24388/0/1390	32171/331/1926
Goodness-of-fit on <i>F</i> ²	1.049	0.890	1.039
Final <i>R</i> indices [<i>></i> 2σ(<i>I</i>)]	<i>R</i> ₁ = 0.1102 <i>wR</i> ₂ = 0.2992	<i>R</i> ₁ = 0.0795 <i>wR</i> ₂ = 0.1680	<i>R</i> ₁ = 0.0478 <i>wR</i> ₂ = 0.1217
<i>R</i> indices (all data)	<i>R</i> ₁ = 0.1214 <i>wR</i> ₂ = 0.3100	<i>R</i> ₁ = 0.1571 <i>wR</i> ₂ = 0.2007	<i>R</i> ₁ = 0.0565 <i>wR</i> ₂ = 0.1268
Largest diff. peak/hole (e.Å ⁻³)	5.464 and -1.799	0.627 and -0.993	2.055 and -0.930

Palladium Complex $2a \cdot 7CH_2Cl_2$

Each molecule of **2a** co-crystallised with seven CH_2Cl_2 solvate molecules, five of which are situated within clefts of HPB moieties and stabilised by two-fold C-H $\cdots\pi$ interactions (C-H $\cdots\pi$ = 2.617-3.377 Å, ESI). The complexes stack to form offset one dimensional columns supported by Pd-Cl \cdots H interactions between a chloro ligand and the benzyl ring of the adjacent pillar (Cl1 \cdots H-Bn = 2.752 Å).

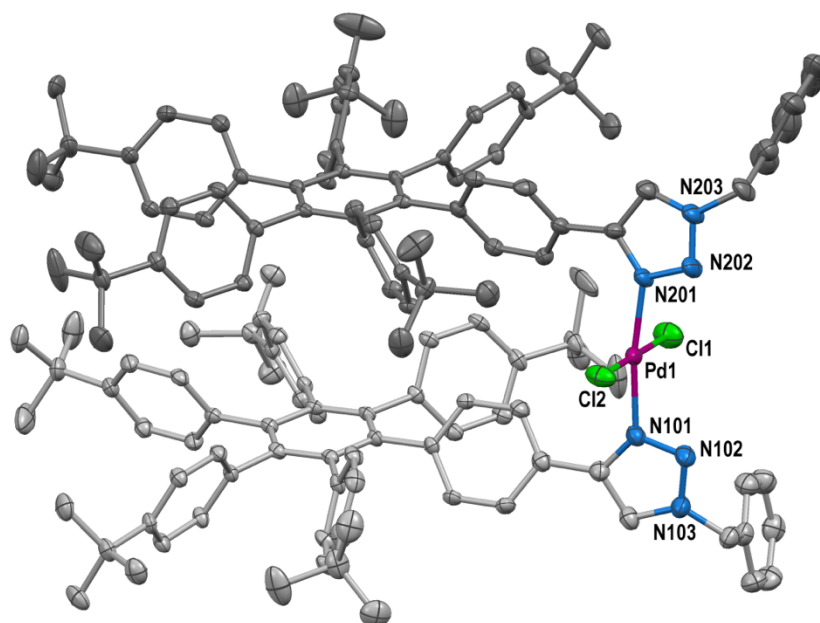


Figure 6.1 ORTEP plot of complex $2a \cdot 7CH_2Cl_2$ with displacement ellipsoids shown at 50% probability. Solvent molecules and hydrogen atoms have been omitted for purposes of clarity.

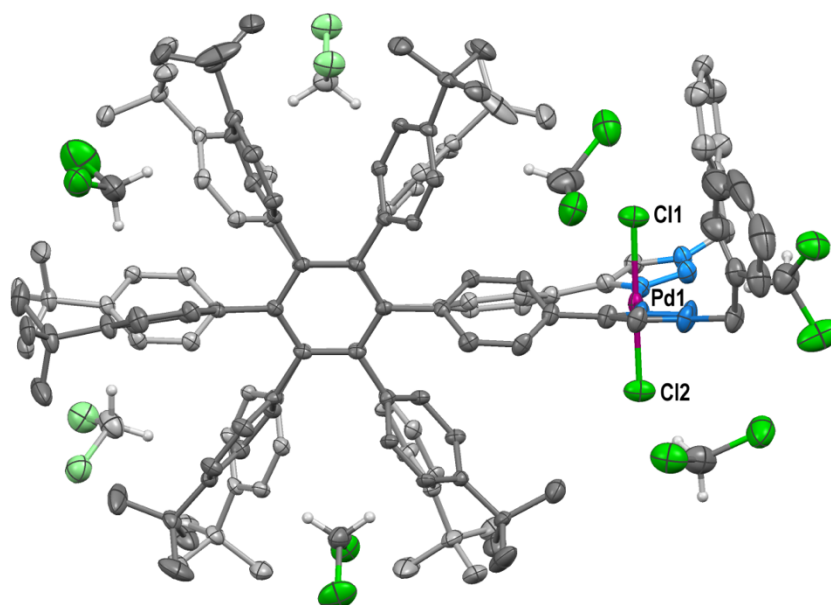


Figure 6.2 ORTEP plot of the asymmetric unit of complex $2a \cdot 7CH_2Cl_2$ with displacement ellipsoids shown at 50% probability. Hydrogen atoms have been omitted for purposes of clarity. Lighter shaded elements are representative of those positioned deeper into the page.

Crystal packing

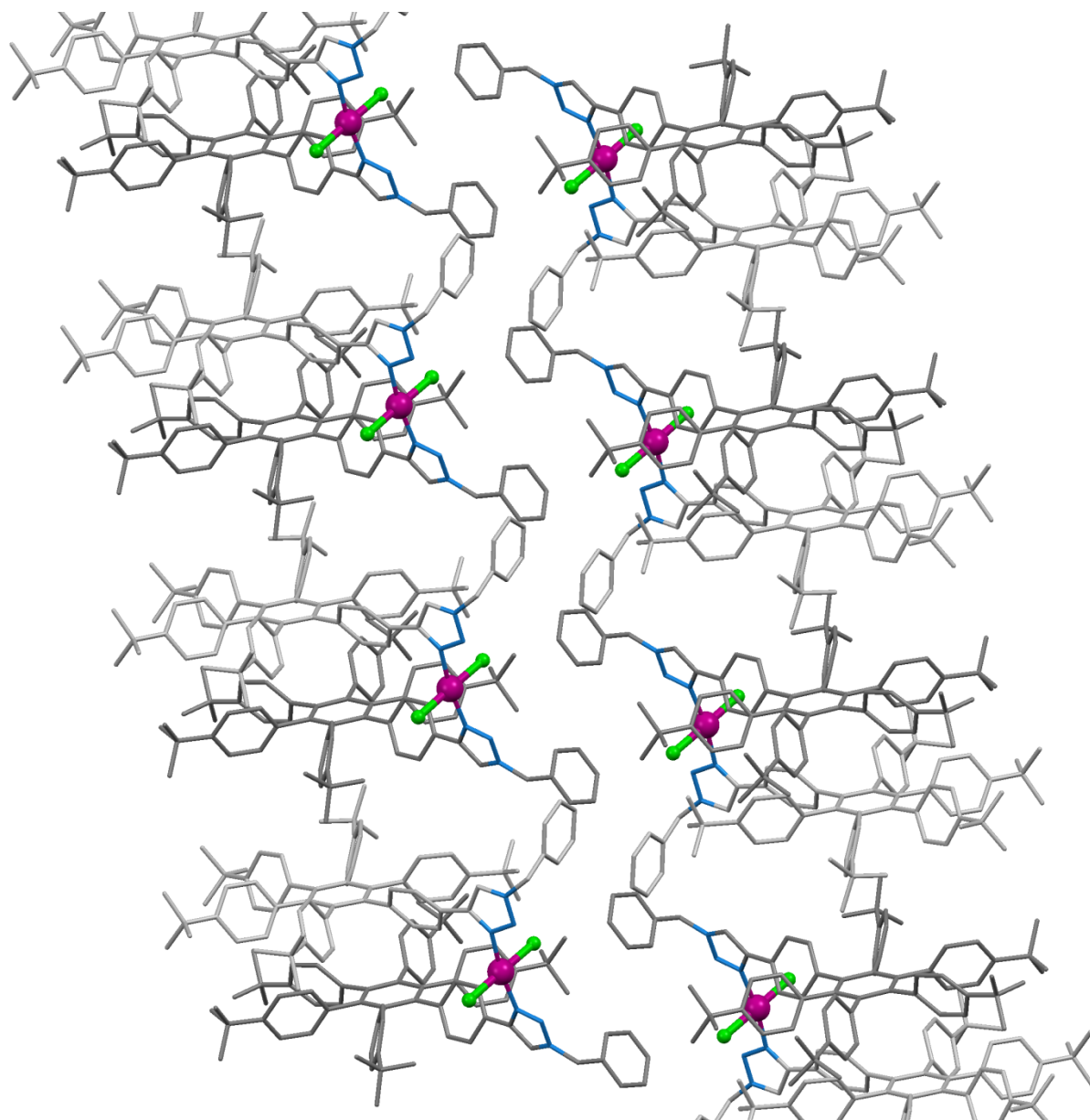


Figure 6.3 Capped-stick representation of complex **2a**·**7CH₂Cl₂**, illustrating the crystal packing arrangement in the form of slipped stacks. The hexaphenylbenzene motifs within each complex are shaded differently for purposes of clarity.

Solvate interactions

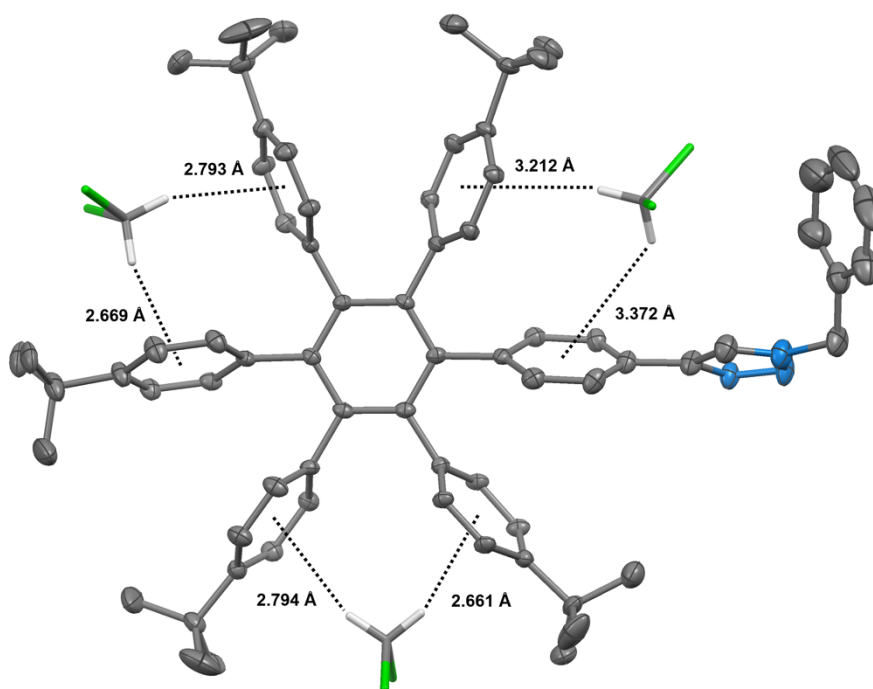


Figure 6.4 ORTEP plot of one of the hexaphenylbenzene ligands of complex **2a**, illustrating the C-H... π interactions that take place between the dichloromethane solvate molecules (represented as capped sticks) and the phenylene rings within the hexaphenylbenzene bay positions. Hydrogen atoms of the ligand have been omitted for purposes of clarity. The displacement ellipsoids are shown at 50% probability.

Palladium Complex **2b**

The HBC moieties are stabilised through offset face-to-face π -interactions facilitated by the π -electron-rich nature of the HBC unit (central ring inter-centroid distance = 3.486 Å). The chloro ligands of **2b** are positioned within bay positions of the HBC units and are stabilised by C-H \cdots Cl interactions (HBC-H \cdots Cl = 2.591-2.996 Å). Within the crystal lattice, the complexes exist as dimers supported by interactions between a benzylic proton and a chloro ligand (C-H103 \cdots Cl1 = 2.779 Å). The dimers closely pack via C-H \cdots π interactions between the HBC cores and peripheral *tert*-butyl substituents of adjacent molecules.

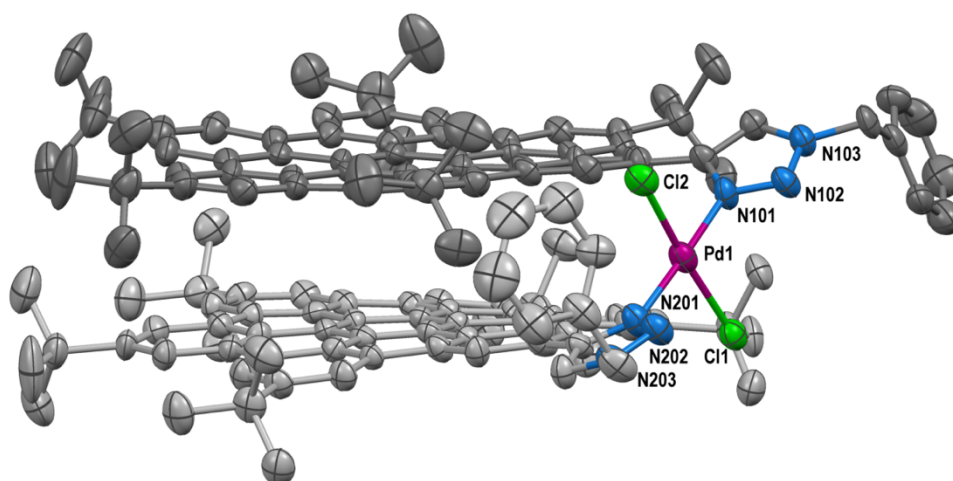


Figure 6.5 The *ORTEP* representation of the X-ray crystal structure of complex **2b** with displacement ellipsoids shown at 50% probability. The hydrogen atoms have been omitted for the purpose of clarity; the carbon atoms of each ligand are shaded differently for the purpose of clarity also.

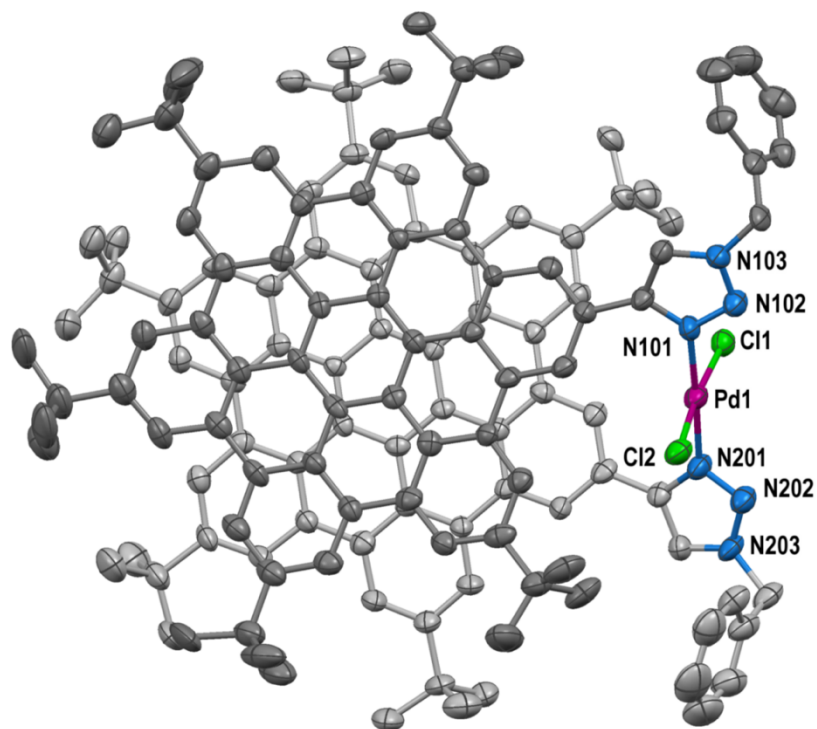


Figure 6.6 The *ORTEP* representation of **2b** with displacement ellipsoids shown at 50% probability, showing a top-down perspective approximately normal to the plane of the hexabenzocoronene moiety. The hydrogen atoms have been removed for the purpose of clarity; the carbon atoms of each ligand are shaded differently for the purpose of clarity also.

Crystal packing

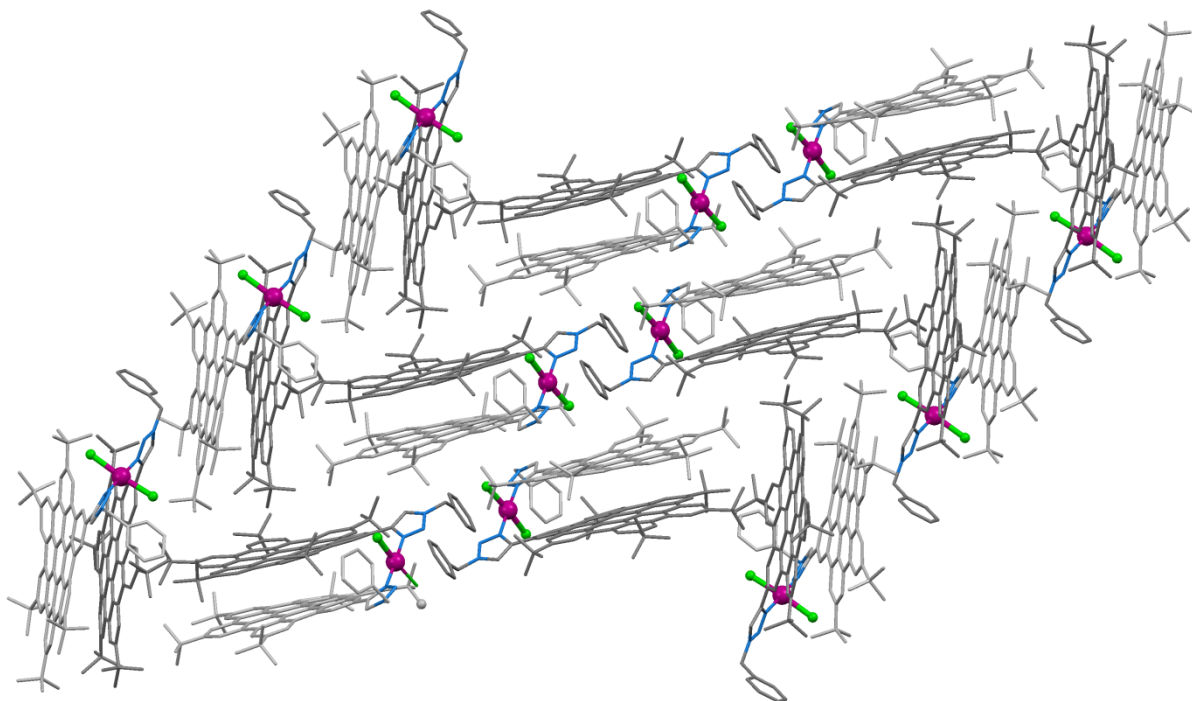


Figure 6.7 A capped-stick representation of the herring-bone-like packing in the crystals of complex **2b**.

Intramolecular interactions

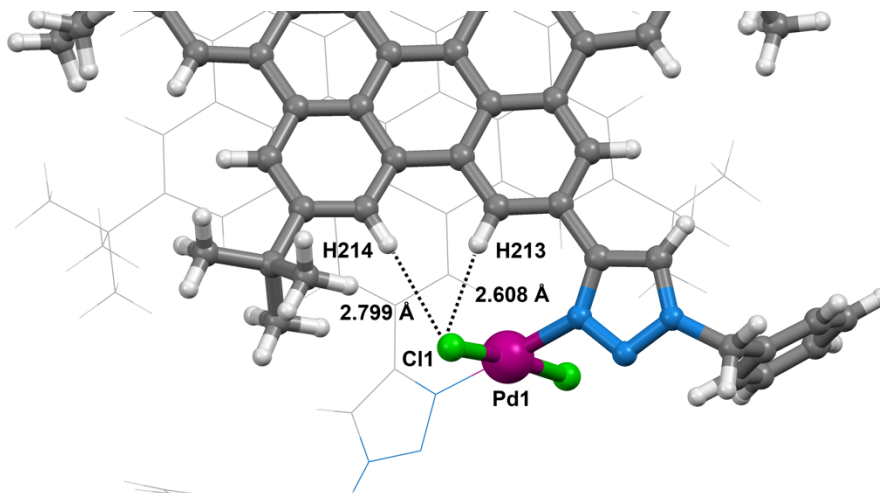


Figure 6.8 Ball and stick representation of the X ray crystal structure of *trans-2b*, illustrating the Cl \cdots H interactions that take place about the bay positions of the HBC substituent. Distances: Cl \cdots H213 = 2.608 Å, Cl \cdots C213 = 3.532(6) Å; Cl \cdots H214 = 2.799 Å, Cl \cdots C214 = 3.749(5) Å

Probe Complex 4b

ORTEP diagrams

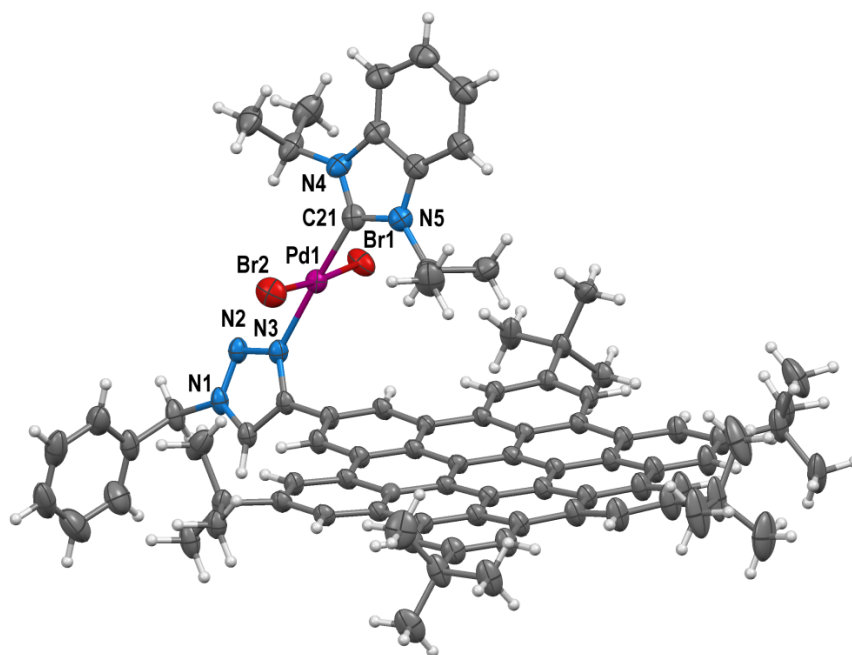


Figure 6.9 ORTEP representation of X-ray crystal structure of complex **4b** with displacement ellipsoids shown at 50% probability.

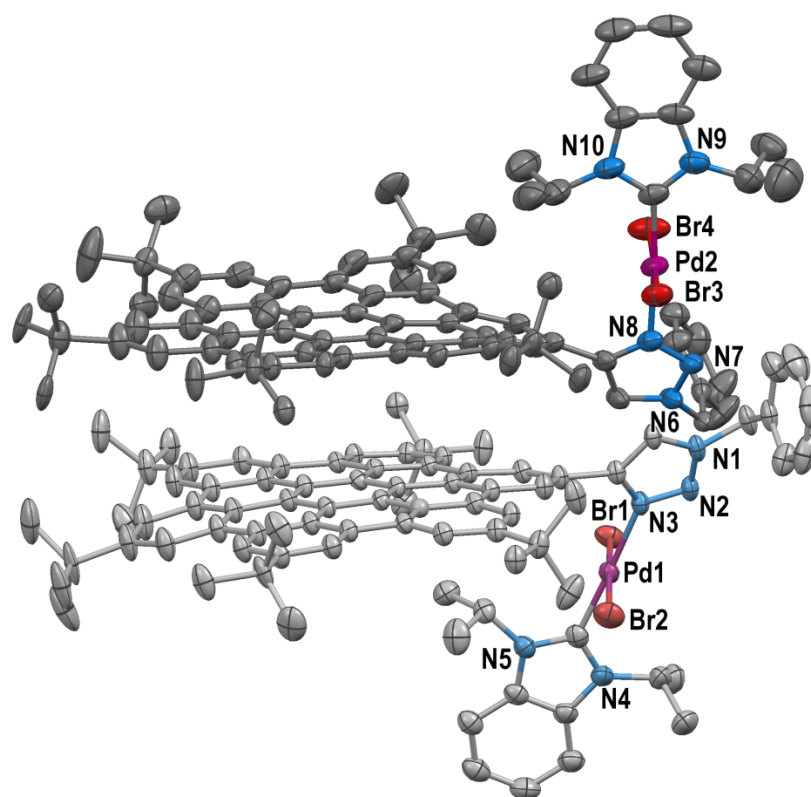


Figure 6.10 ORTEP representation of the asymmetric unit of the X ray crystal structure of **4b** with the displacement ellipsoids shown at 50% probability. The hydrogen atoms have been omitted for the purpose of clarity. The two molecules comprising the asymmetric unit are shaded differently for clarity.

Crystal packing

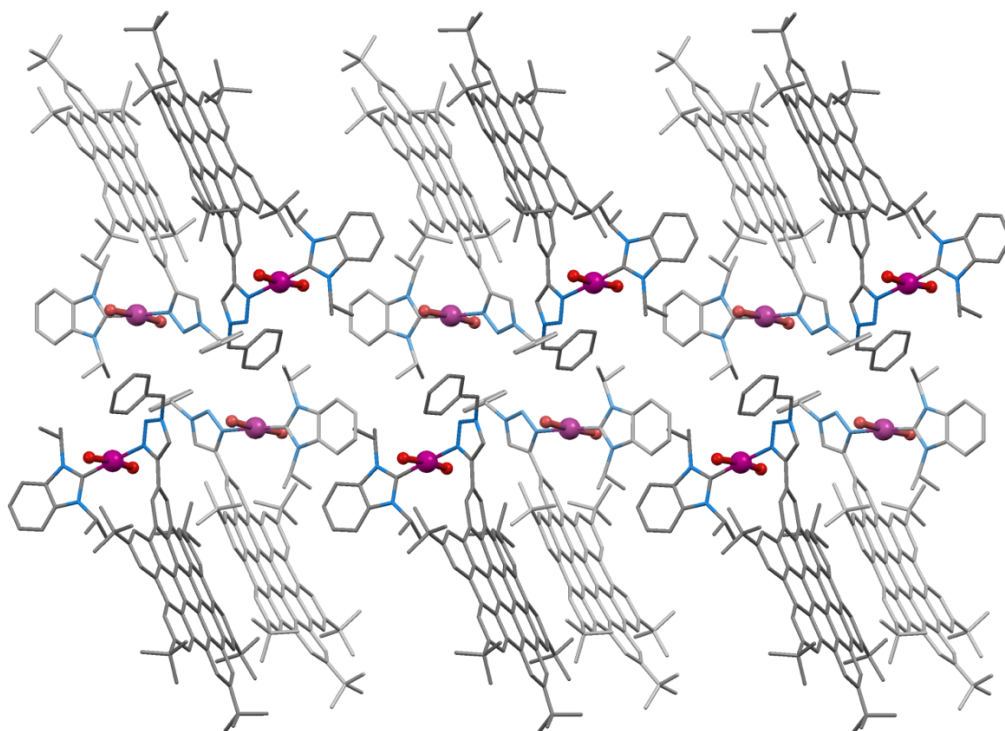


Figure 6.11 A capped stick representation of the lattice in the crystal of **4b**.

7 Molecular Modelling

Molecular modelling calculations of *cis-2a-c* were carried out using the Spartan '06 software package employing the Merck Molecular Force Field (MMFF) method, to geometrically optimise the structures. The models were optimised with ligand-Pd-ligand angles constrained at 90° about the palladium(II) centres until a minimum was reached. The constraints were subsequently removed and minimised again until no change was observed.

From these structures there is no appearance of significant geometric strain about the palladium(II) centres. For complexes *cis-2a* and *cis-2b*, however, the organic groups appear to bend out of planarity in order to satisfy metal-ligand bonding geometries. The HPB groups of *cis-2a* and *trans-2b* bow slightly toward each other, close to the coordination sphere, whereas the HBC groups of *cis-2b* appear to curve in unison toward the coordination sphere, to satisfy the coordination geometry and the favourable face-to-face π -interactions. The model of *trans-2b* is reflective of the X-ray crystal structure in which the HBC groups bow inwards to maximise face-to-face π -interactions.

The relative energies of the *cis*- and *trans*-geometries of each complex is tabulated below:

Table 7.1 Comparison of *cis*- and *trans*- energies for complexes **2a-c**.

Complex	<i>trans</i> - energy (kJ mol ⁻¹)	<i>cis</i> - energy (kJ mol ⁻¹)	Energy difference (kJ mol ⁻¹)
2a	2370	2385	15
2b	2598	2633	35
2c	304	291	-13

These results suggest that both configurations of each complex are energetically accessible, without the presence of major steric strain.

Cis and *trans* isomers of HPB complex 2a

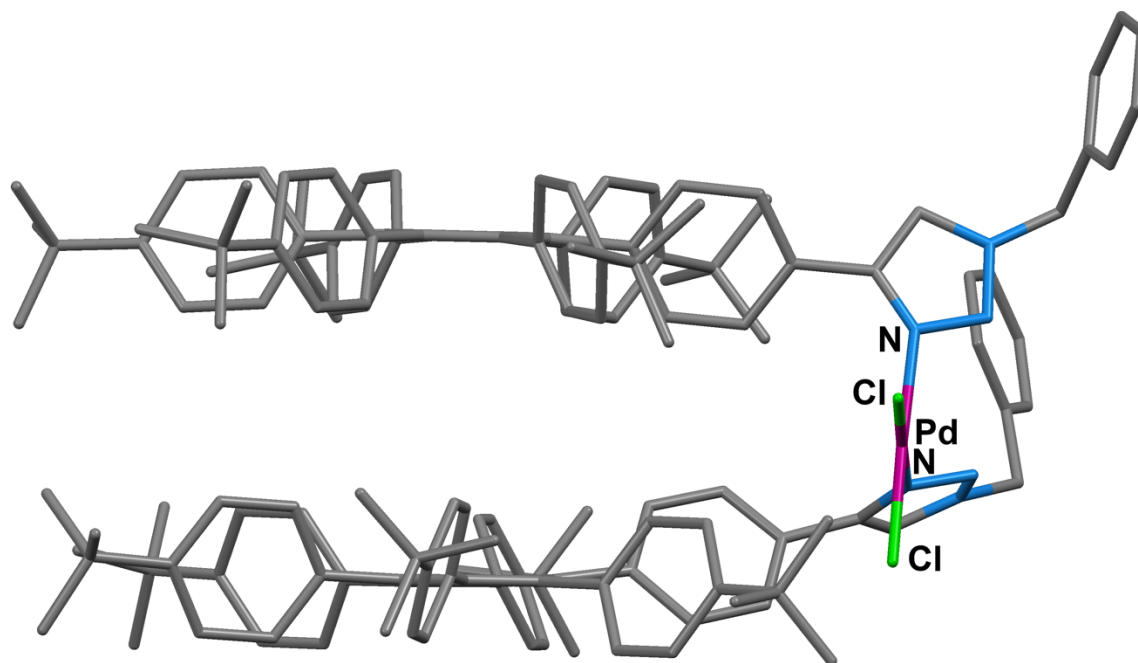


Figure 7.1 Energy-minimised structure of palladium complex *cis*-2a.

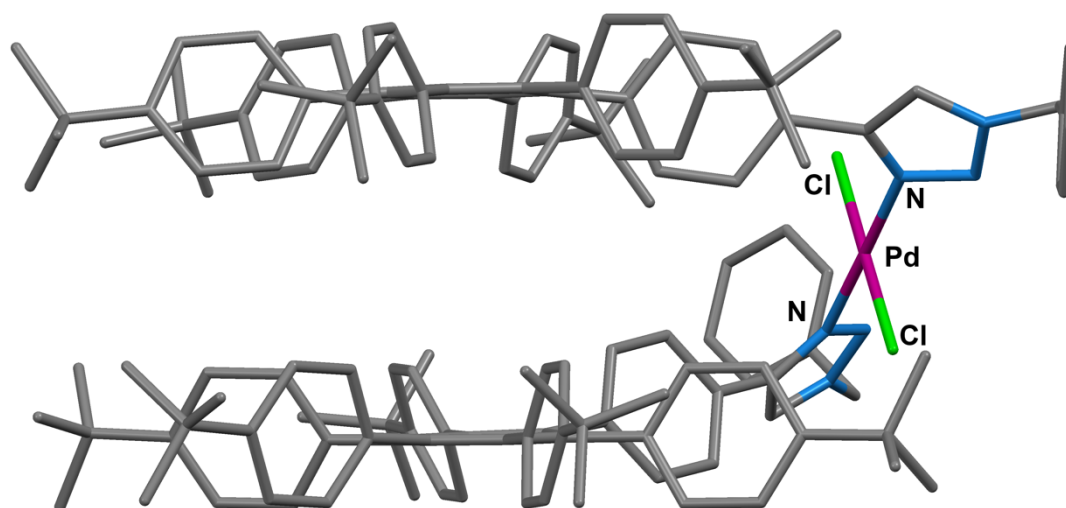


Figure 7.2 Energy-minimised structure of palladium complex *trans*-2a.

Cis and *trans* isomers of HBC complex 2b

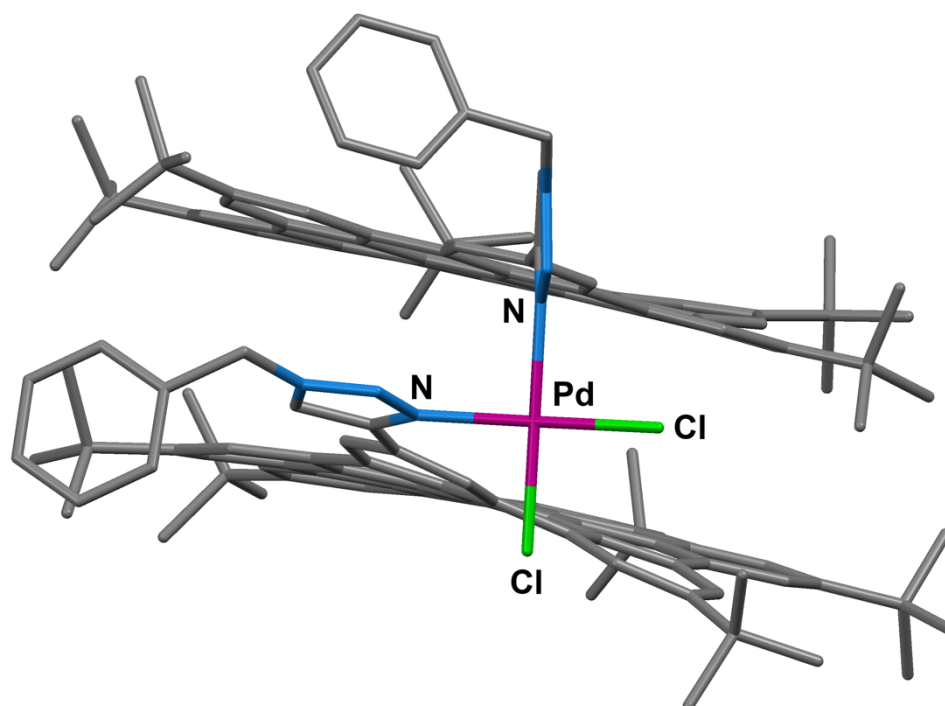


Figure 7.3 Energy-minimised structure of palladium complex *cis*-2b.

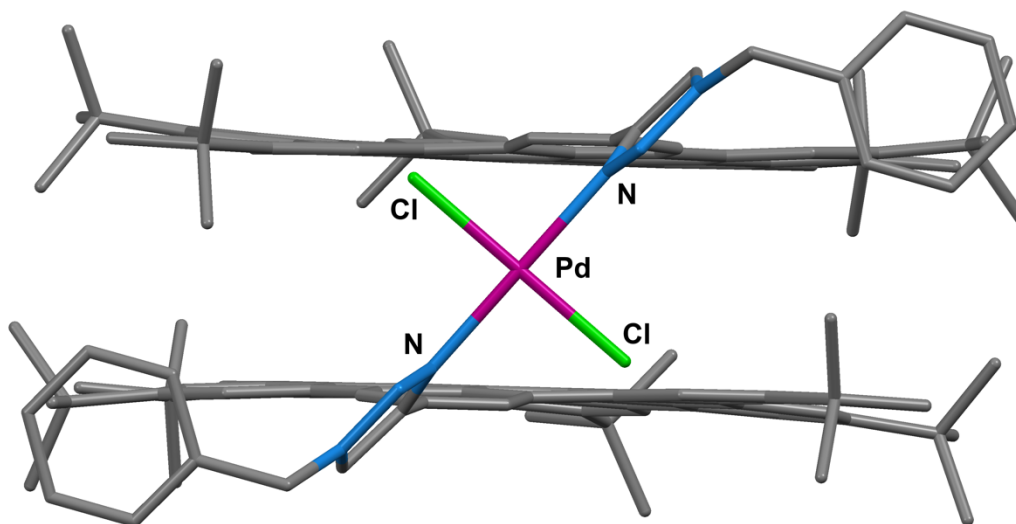


Figure 7.4 Energy-minimised structure of palladium complex *trans*-2b

Cis and *trans* isomers of model complex 2c

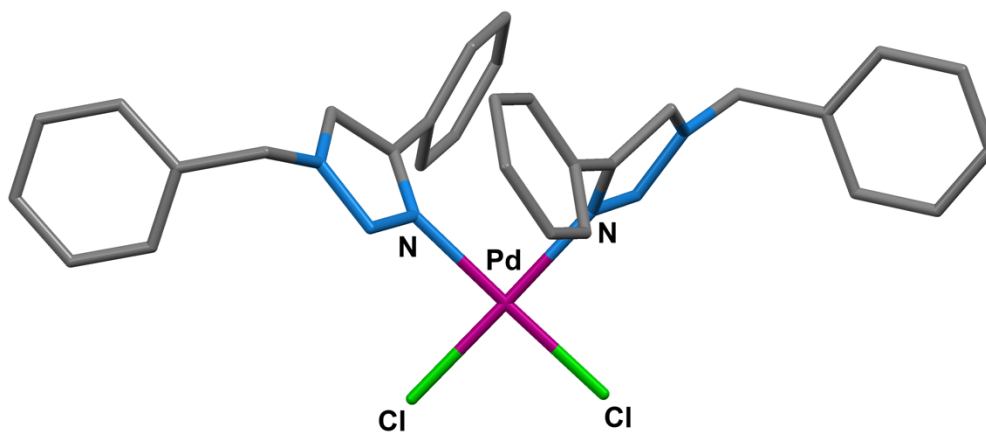


Figure 7.5 Minimised energy structure of palladium complex *cis*-2c.

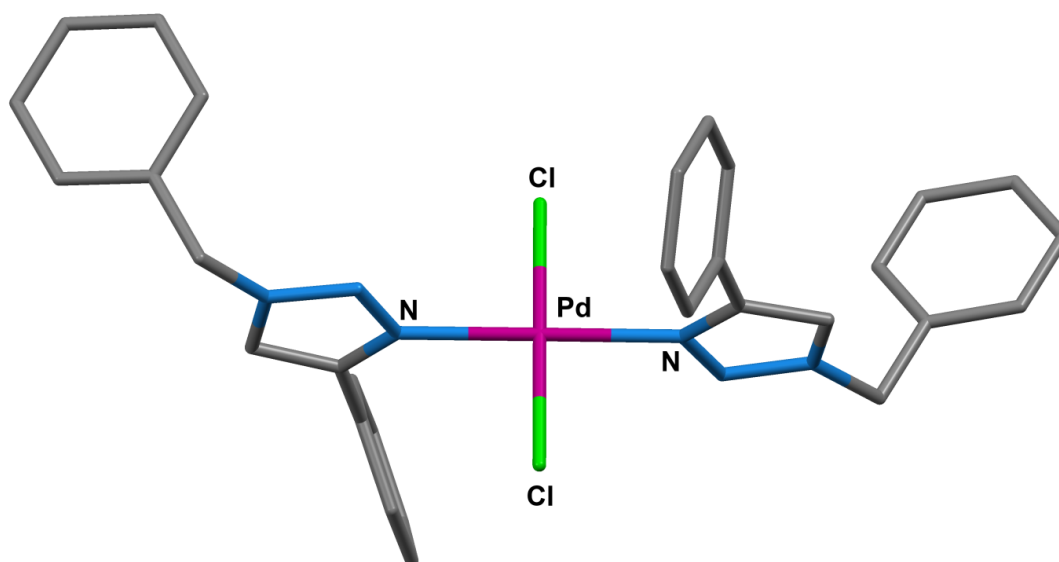


Figure 7.6 Minimised energy structure of palladium complex *trans*-2c

8 Catalyst Screening

¹H NMR Studies

All the reactions that were performed to test the catalytic activity of complexes **2a**, **2b**, model **2c**, and **3** in the Suzuki-Miyaura reaction were monitored via ¹H NMR spectroscopy.

The samples were prepared accordingly:

After the reaction mixture had ceased stirring and the layers had separated (1 min), 0.2 mL aliquots were removed from the organic (toluene) layer (18 mL) at t = 0 hr, and every hour afterwards until no change in conversion was observed. The aliquots were passed through a small plug of Celite, and washed through with dichloromethane (3 x 1 mL). The solvent was removed *in vacuo* and a NMR sample was prepared from the remaining residue and immediately measured. The product was measured against the internal standard 1,3,5-trimethoxybenzene.

Based on comparison of the isolated yields with the respective conversions gathered via ¹H NMR spectroscopy, the method appears to have an associated uncertainty of ±5%.

3,5-Dimethoxybiphenyl

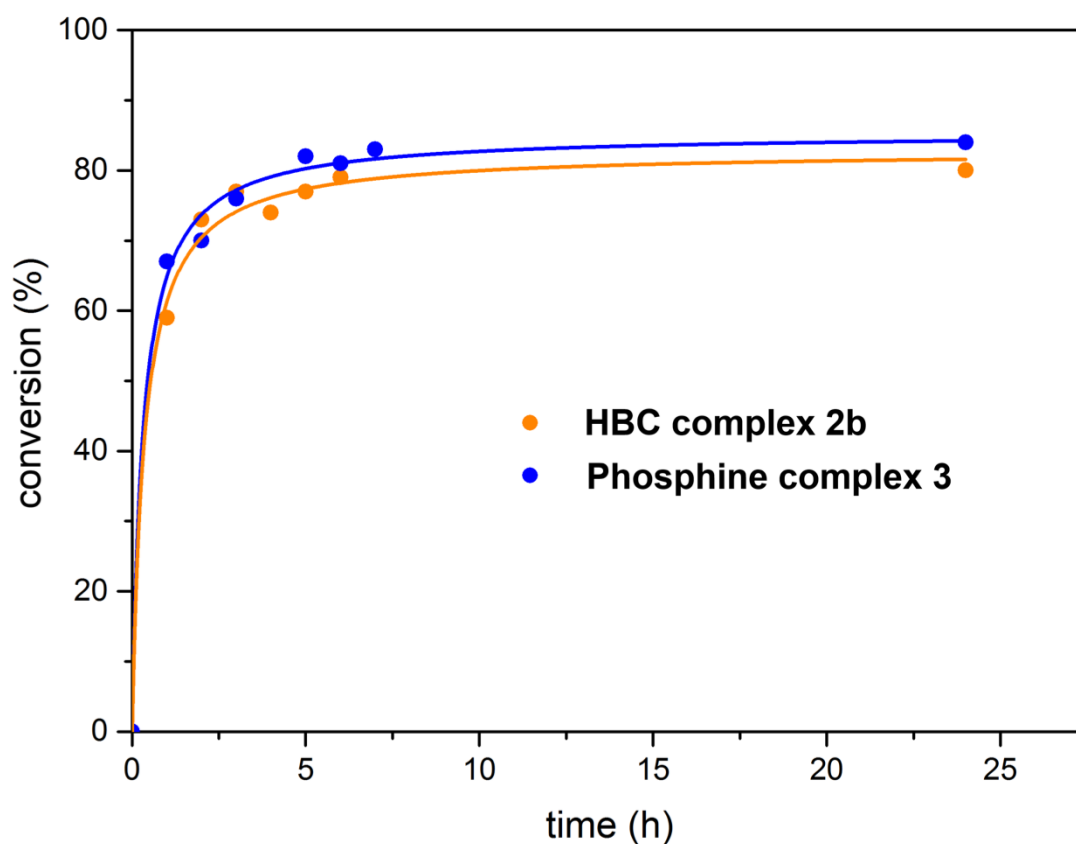


Figure 8.1 ¹H NMR monitoring of the catalysed formation of 3,5-dimethoxybiphenyl with complexes **2b** and **3** in the Suzuki-Miyaura reaction.

4-Acetylbiphenyl from 4-Chloroacetophenone

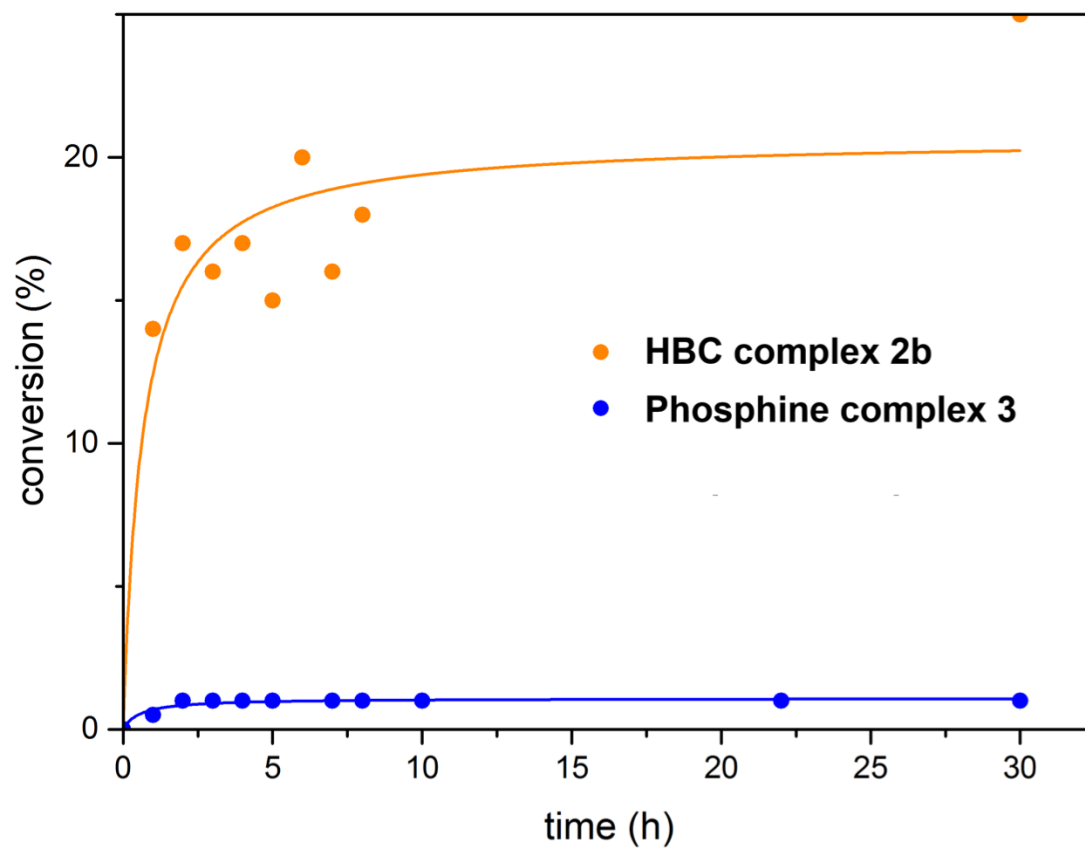


Figure 8.2 ^1H NMR monitoring of the catalysed formation of 4'-acetylbiphenyl with complexes **2b** and **3** in the Suzuki-Miyaura reaction.

9 References

- 1 H. E. Gottlieb, V. Kotlyar and A. Nudelman, *J. Org. Chem.*, 1997, **62**, 7512.
- 2 D. Nolan, B. Gil, F. A. Murphy and S. M. Draper, *Eur. J. Inorg. Chem.*, 2011, **2011**, 3248.
- 3 A. B. S. Elliott, R. Horvath, X.-Z. Sun, M. G. Gardiner, K. Müllen, N. T. Lucas, M. W. George and K. C. Gordon, *Inorg. Chem.*, 2016, **55**, 4710.
- 4 M. L. Gower and J. D. Crowley, *Dalton Trans.*, 2010, **39**, 2371.
- 5 M. Rimoldi, F. Ragaini, E. Gallo, F. Ferretti, P. Macchi and N. Casati, *Dalton Trans.*, 2012, **41**, 3648.
- 6 F. A. Murphy and S. M. Draper, *J. Org. Chem.*, 2010, **75**, 1862.
- 7 I. J. S. Fairlamb, A. R. Kapdi and A. F. Lee, *Org. Lett.*, 2004, **6**, 4435.
- 8 L. Ackermann, C. J. Gschrei, A. Althammer and M. Riederer, *Chem. Commun.*, 2006, 1419.
- 9 S. M. McNeill, D. Preston, J. E. M. Lewis, A. Robert, K. Knerr-Rupp, D. O. Graham, J. R. Wright, G. I. Giles and J. D. Crowley, *Dalton Trans.*, 2015, **44**, 11129.
- 10 H. V. Huynh, Y. Han, R. Jothibasur and J. A. Yang, *Organometallics*, 2009, **28**, 5395.
- 11 Agilent (2014), CrysAlis PRO version 1.171.36.28, Agilent Technologies Ltd, Yarnton, Oxfordshire, UK.
- 12 G. Sheldrick, *Acta Cryst. A*, 2008, **64**, 112; G. M. Sheldrick (1998), SHELX-97, University of Göttingen: Germany.
- 13 L. J. Barbour, *J. Supramol. Chem.*, 2001, **1**, 189.